CHALMERS
UNIVERSITY OF TECHNOLOGY

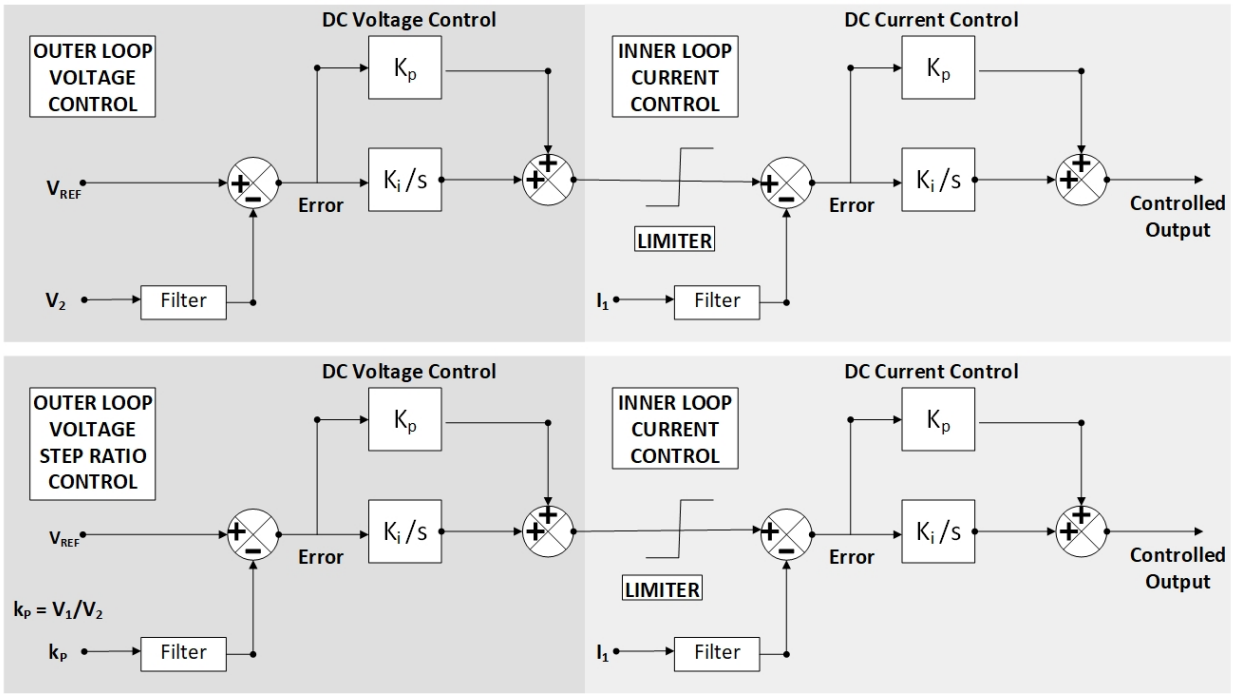

On Control Strategies of Series Embedded DC/DC Converters in MTDC Grids

Verification of Control Strategies for DC/DC Converters on the CIGRE DC Grid Test System

Master's Thesis in Electric Power Engineering

ARUN DILIP KHILNANI

Department of Electrical Engineering
CHALMERS UNIVERSITY OF TECHNOLOGY
Gothenburg, Sweden 2019

Master's thesis 2019

On Control Strategies of Series Embedded DC/DC Converters in MTDC Grids

Verification of Control Strategies for DC/DC Converters on the CIGRE DC Grid Test System

Arun Dilip Khilnani

CHALMERS
UNIVERSITY OF TECHNOLOGY

Department of Electrical Engineering
Division of Electric Power
Chalmers University of Technology
Gothenburg, Sweden 2019

On Control Strategies of Series Embedded DC/DC Converters in MTDC Grids
Verification of Control Strategies for DC/DC Converters on the CIGRE DC Grid Test System
ARUN DILIP KHILNANI

Supervisors: Gustavo Pinares and Massimo Bongiorno, Department of Electrical Engineering
Examiner: Massimo Bongiorno, Department of Electrical Engineering

Master's Thesis 2019
Department of Electrical Engineering
Division of Electric Power
Chalmers University of Technology
SE-412 96 Gothenburg
Telephone +46 31 772 1000

Cover: Outer Loop for Voltage Control and Outer Loop for Voltage Step Ratio Control

Typeset in LaTeX
Printed by Chalmers Reproservice
Gothenburg, Sweden 2019

On Control Strategies of Series Embedded DC/DC Converters in MTDC Grids
Verification of Control Strategies for DC/DC Converters on the CIGRE DC Grid Test System
ARUN DILIP KHILNANI
Department of Electrical Engineering
Chalmers University of Technology

Abstract

Due to increasing load demands and the need to integrate bulk power generated from newer offshore RES based power plants into the existing AC grid, many challenges in maintaining stability and grid expansion are now foreseen. Given the AC losses, economics and other factors in long distance power transmission, HVDC technology is now being preferred for expanding the grid further. Till now, HVDC links have been developed in a point-to-point configuration, but would require to be integrated into smaller DC networks initially, before a gradual expansion into a MTDC grid can be made possible. This MTDC grid would use the existing AC grid as a substrate and would consist of many AC & DC subsystems at different voltage levels.

RES based offshore plants take many years to develop and as DC cable ratings rise by tens of kilo-volts at each iteration of the HVDC technology, it is quite plausible that geographically adjacent offshore power plants could have different DC voltage ratings. Therefore, the formation of a MTDC grid could require a DC/DC converter (analogous to an AC transformer in an AC grid) that can primarily match different DC link voltages and integrate them into a meshed DC grid. The DC/DC converter could be further used for power regulation over the DC grid, probably in conjunction with VSC based control.

In point-to-point HVDC configurations and meshed DC grids, control strategies on VSCs for DC power flow regulation are well understood. However, since MTDC grid topologies are theoretical, control strategies on series embedded DC/DC converters for DC power flow control in steady state are yet to be studied. Particularly, control strategies developed on DC/DC converters in MTDC grids for DC power flow control in steady state, following a (n-1) DC link contingency criterion, independent of VSC based control, are yet to be developed.

In the thesis, a DC side equivalent model of the CIGRE DC Grid Test Model is developed to study DC power flow on the MTDC grid in steady state. The control strategies are exclusively developed on the series embedded DC/DC converters for voltage and current control, following a (n-1) contingency criterion. Further, various scenarios like variation of VSC input power, step responses from the DC/DC converters and implementation of additional DC links into the DC grid are studied as well.

Keywords: MTDC, HVDC, VSC, Control Strategies, DC/DC converters, DC Power Flow, CIGRE DC Grid Test System

Acknowledgements

The scholarship support provided by the Swedish Institute (SI Scholarships) is gratefully acknowledged.

I would like to express sincere gratitude to my supervisor Gustavo Pinares for his constant support and persistence during the development of the thesis. Many thanks to my examiner Massimo Bongiorno for introducing me to this topic, for his guidance and critical analysis of the thesis as well.

Arun Dilip Khilnani, Gothenburg, February 2019

Contents

List of Figures

List of Tables

1
Introduction

This chapter describes the background, motivation, aim, methodology and scope of the thesis. The intended contribution of the thesis is presented as well. Lastly, an outline of the sections of this report is listed.

1.1 Background

A possible vision of electricity in the world is of a *Global Grid* that is envisaged to integrate all continental electrical grids into a single grid structure. This development will possibly connect major power plants with major load centres in the world, thereby creating a global trade market for electricity. However, this vision will first require grids to evolve from being country-wise to continental structures, before a further integration of continental grids into a single *Global Grid* can be made possible. This continental *SuperGrid* in Europe is envisaged as shown in Figure 1.1, and could be made possible by integration of major load centres (such as London, Paris & Stockholm) with offshore wind and solar power plants from remote locations (such as the Baltic Sea for wind power and Sub-Saharan deserts for solar power) [1].

In the coming decades, it is expected that almost all new electrical generation will utilise Renewable Energy Source (RES) based power plants, as the share percentage of the same is expected to grow exponentially [2]. There is, in particular, large untapped energy available offshore where most of the large MW *bulk capacity* RES based power plants are planned, away from load centres. This bulk power will require to be integrated into the existing AC grid, which would pose many challenges on the existing AC grid stability [3]. Moreover, due to the regulatory norms requiring electrification of offshore Oil & Gas platforms to be electrified completely from RES based power plants [4], many challenges in the integration of this bulk power into the existing AC grid are now foreseen.

Considering the lower voltage level required as compared to DC, AC was seen as a favourable option for rapid expansion of the grid in the previous century. With growing load demands now and the economical factors over long distance transmission, expanding the grid using only AC technology is no longer seen as a favourable option [4]. Correspondingly, the other option of using DC technology for long distance transmission of electrical power is being explored extensively, both by the academic community as well as the industry [5]. Figure 1.2 shows a typical graph

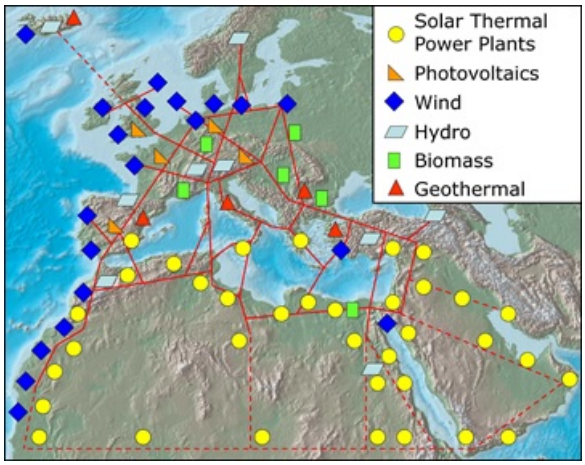

Figure 1.1: Conceptual European SuperGrid [1].

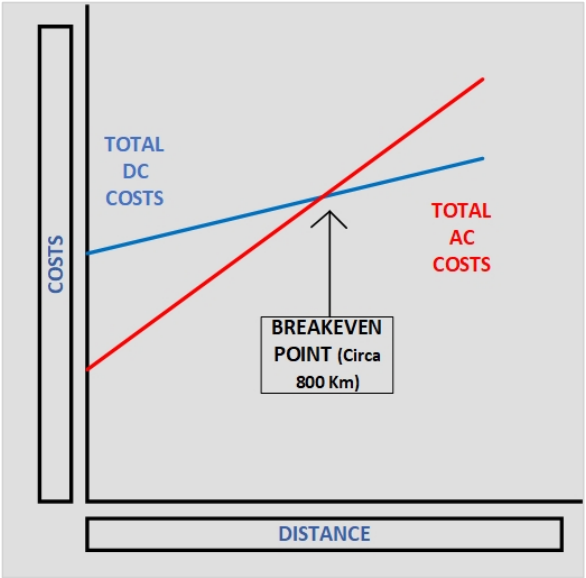

Figure 1.2: Cost comparison of AC and DC over transmission distance [1].

that describes the initial costs in developing AC & DC substations and the increase of cost along the length of the transmission lines. It is observed that at some distance over the long transmission links, DC technology becomes more economical than AC. However, the same is subjective to various factors related to cost and type of project being developed and load forecasting as well. Hence, given the vision of an European *SuperGrid*, developing DC grids over AC grids substrates is seen as a favourable vision and further research is motivated.

Recent developments in High Voltage DC technology along with advancements in semiconductor technology have led to development of Voltage Source Converters (VSC) based High Voltage DC Links (HVDC), commonly termed as VSC based HVDC systems. A block diagram of a VSC based HVDC systems is shown in Figure 1.3. This configuration utilises two VSCs & a Bipole HVDC link and is

commonly termed as a Point-to-Point HVDC Transmission system. In this configuration, power is converted from AC to DC (rectification) at the sending end, transmitted on the Bipole DC link, and then converted back from DC to AC (inversion) at the receiving end. The typical control strategy is that the sending end VSC controls the DC Link voltage, while the receiving end is used for power control [7]. This flexibility in controlling the power over the DC link is seen as a major advantage in using HVDC over AC technology.

Currently, VSC based HVDC links have been commissioned in a point-to-point based configuration to transfer power from an offshore located RES power plants to onshore load centres. However, the possible vision of an European *SuperGrid* will require integration of many such HVDC links into an integrated network [8]. Hence, there is strong motivation to develop a DC grid that has multiple interconnections of HVDC links, further forming a meshed HVDC network. These HVDC links will initially be developed into smaller DC networks which could further interconnected into a meshed grid. This meshed grid is termed as Multi Terminal HVDC grid (MTDC grid) and is envisaged to be developed with the existing AC grid as a *substrate*. (A detailed description of an MTDC grid and its various configurations particular to the thesis is given in Chapter 2 of this report.)

Considering that the development of an RES based power plant usually takes many years to be fully functional, the development of an MTDC grid is foreseen to have many challenges. Particularly, technical challenges concerning the formation of a MTDC grid with a specific topology that would be a gradual development of smaller DC networks will be of prime importance. The existing and planned VSC based HVDC Links are mainly point-to-point configurations and are usually of different voltage ratings and grounding schemes [9]. The integration of these HVDC links into a MTDC grid will require a device that can allow primarily the interconnection of DC systems of different voltage ratings, control DC power flow and prevent overloading of DC Links in case of contingencies. This DC level controller, termed as a *DC/DC converter*, is proposed to fulfil these functions, analogously to an AC transformer in an AC Grid. The DC/DC converters are expected to perform many functions over an MTDC grid [10] :

- Step-UP and Step-DOWN the DC voltage over the HVDC links, so as to integrate them into a common MTDC grid.

- Regulation of DC power flow by current and voltage control on the MTDC grid.

- Acting like a DC circuit breaker.

- Providing galvanic isolation to the HVDC links, if needed.

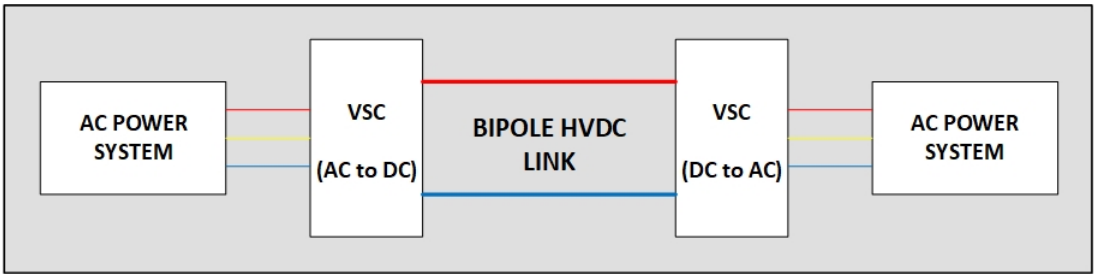

Figure 1.3: VSC based HVDC system [7].

Concerning DC/DC converters, several authors have investigated their applications in MTDC grids from different perspectives. These include developing suitable topologies for DC/DC converters that could be applied in MTDC grids. In case of point-to-point HVDC, the control of power over the HVDC links is well understood as the VSC converters support bidirectional power flow. The DC power flow over the HVDC links in case of contingencies on the AC side is researched as well. Further, as MTDC grids are yet to be developed, to understand DC power flow control and the control strategies developed specifically on VSCs, much research is published.

Hence, the focus of this thesis is to investigate the application of DC/DC converters in meshed and radial configurations of MTDC grids and to define suitable control strategies on them. Concerning the same, a literature review is described in the next section.

1.2 Literature Review

In this section, control strategies for MTDC grids using VSC based control are reviewed. These mainly include control strategies using droop control techniques for voltage and current to maintain stability on the DC side. Further, concerning stability studies for DC power flow using AC parameters are described as well. Investigations about the topological development of DC/DC converters are reviewed concerning their suitability for MTDC applications.

In [9] a brief review of topologies of DC/DC converters that could be applied for interconnecting independent HVDC links of different voltage ratings into an MTDC grid is published. The publication recommends topological development of an AC-transformer coupled with a *DC/AC/DC* converter; simulations conducted are over a prior CIGRE DC Grid Test Model, with no series embedded DC/DC converters. Further assessment of DC/DC converter toplogies in [11] shows that a DC/DC converter with a unity conversion ratio can be used to integrate HVDC links of different voltage levels into a MTDC grid. The paper also concludes that a resonant DC/DC

converter that utilises a capacitor-arm between two converters is best suited for the same. Feasibility of DC transmission networks as cited in [12] show that a practical challenge in developing MTDC grids is lack of an integrated grid protection system and a fast acting HVDC circuit breaker. The paper further argues that, as compared to AC systems in which the power flow is governed by slow-acting governors, the DC systems shall need fast-acting converters as tripping of the DC Links will be based using thyristors. Further, the time constants for the DC grid response will be of two orders of magnitude smaller which would complicate the applied control strategies, but could make power optimisation better.

Concerning DC power flow control over the MTDC grids, in [13], a voltage droop control strategy over the MTDC grid is introduced, such that it maintains the DC grid voltage close to its nominal value in contingency conditions. Further, stability analysis of voltage droop controller in MTDC grid is investigated in [14], wherein small signal stability of the VSC is analysed for droop control schemes. Further, power dependent droop control strategies for MTDC grids are designed and tested in [15], wherein, a modified droop control is introduced which is better suited for dynamic responses of the power system. Precise control of power flow in MTDC grids using voltage droop control is understood in [16]. This paper also concludes that dips in current & voltage over the DC links and converter losses should also be taken into account while considering stability analysis of the DC power flow. Control of remote MTDC grid using AC frequency control is understood in [17], wherein frequency variations on AC side are used to control the DC power flow. Some research regarding DC grid management of MTDC grids for robustness with respect to integration of large wind farms is also presented in [18].

Requirements for DC/DC converters in HVDC grids have been investigated extensively. It is found that the suitability of DC/DC converters depends on voltage ratios, power flow direction, overall system configurations and the need for galvanic separation [10]. Considering these aspects, many topologies have been proposed for DC/DC converters *(Front-to-Front DC/AC/DC, Transformer-Coupled DC/AC/DC, LCC/VSC DC/AC/DC, Modular DC/DC, Modular Resonant DC/DC)* for both High and Medium voltage levels and reviews of the same have also been published [19]. The literature review further showed that the development of the DC/DC converter topology was guided by the topological advantage offered by one design over the other, while the control advantage was not considered. In other words, the DC/DC converter topologies developed do not consider control flexibility or adaptability into consideration and only consider hardware advantages.

1.3 Motivation

It was found that several studies concerning the development of control strategies to be implemented in VSC based HVDC systems have been performed. These studies use either a 4-terminal or a 5-terminal meshed HVDC network to test control strategies without considering the existence of series embedded DC/DC converters. Some studies utilise a former CIGRE DC Grid Test Model that does not include series

embedded DC/DC converters as well. These control strategies are developed with an understanding of bi-directional power flow, with one VSC performing voltage control, while the other for power control. Moreover, studies concerning the topological design of DC/DC converters have been extensively performed, while studies concerning the utilisation of DC/DC converters in control of MTDC grids are not found extensively.

It is not exactly understood how DC power flow over an independent MTDC grid will be regulated without any control from the VSCs, but only through the control strategies developed on the series embedded DC/DC converters. The control strategies for DC power flow control and voltage control are not investigated considering the existence of many DC/DC converter topologies. To further examine and understand the same, considering if an MTDC grid has n DC links, the DC power flow regulation and maintaining grid stability using an (n-1) contingency criterion, with control strategy applied only on series embedded DC/DC converters yet remains to be investigated.

1.4 Aim

The objective of this master thesis is to propose and decide suitable control strategies over DC/DC converters that are series embedded into a MTDC grid. In particular, control strategies that aim for control and stability of power flow over the DC links for current and voltage control following a (n-1) contingency criterion will be developed. The test grid used will be the CIGRE DC Grid Test Model, that is a benchmark model developed by the CIGRE Work Groups B.57 & B.58. The CIGRE DC Grid Test Model used is the latest version, with two series embedded DC/DC converters.

1.5 Scope

The following activities are performed as part of the Master Thesis:

- Literature review on VSC based control strategies applied on MTDC grids, on DC grid stability and functional design of DC/DC converter topologies.

- The benchmark model developed by CIGRE Work Groups B.57 & B.58 is used for modelling the DC Side with certain limitations. Further, an averaged model of a DC/DC converter is developed in PSCAD.

- Control strategies for DC/DC converters that are series embedded in MTDC grids are developed for steady-state analysis by applying the (n-1) contingency criterion on the DC side developed model.

- Three types of control strategies are developed - Inner Loop for current control, Outer Loop for voltage control using voltage input and Outer Loop for voltage control using voltage step ratio.

- Further analysis of the control strategies in cases of selective control strategies, modification of voltage step ratio control, varying power inputs to the MTDC grid, DC/DC converter power set-point responses and implementation of additional DC Links are also conducted.

1.6 Contribution of the Thesis Work

The thesis is intended to help understand DC power flow and its control over an MTDC grid using control strategies developed in case of (n-1) contingency conditions. Control strategies over the DC/DC converters with selective control loops to maintain DC Grid stability and other conditions such as variance in power input to the MTDC grid, modification of voltage step ratio control when the MTDC is connected to weak DC voltages at VSC output, step responses from the DC/DC converters and implementation of additional HVDC links for increasing DC grid robustness are developed. The thesis will help understand how possible integration of control structures of VSCs and DC/DC converters can be further investigated and developed. Moreover, studies regarding the functionality of DC/DC converters can also be used as inputs to hardware design.

1.7 Outline for the Thesis Work

This thesis work is divided into seven chapters.

- **Introduction** : This chapter has described the background, motivation, aim, methodology and the scope of the thesis. The intended contribution of the thesis has been presented as well. Lastly, an outline of the sections of this report is listed here.

- **About VSC-HVDC Systems and MTDC Grids** : This chapter describes the MTDC grid topologies that are envisaged to be built using existing AC grids as substrates. A brief introduction into VSC based HVDC configuration and types of DC links applied is given as well. Lastly, motivations to develop a DC/DC converter from a control perspective are presented.

- **DC Side Model of CIGRE DC Test Grid** : This chapter describes the CIGRE DC Grid Test Model developed by Work Groups B4-57 and B4-58. Its implementation for studying DC power flow is described. The averaged model of the series embedded DC/DC converters developed is explained as well. Further, a steady state analysis of DC power flow on the developed model is presented.

- **Control Loops Developed** : This chapter describes the Inner and Outer control loops developed for DC power flow and their implementation over the developed DC side model of the CIGRE DC Grid Test Model.

- **Steady State Contingency Analysis** : This chapter presents the results of contingency analysis performed in the developed DC side model of the CIGRE DC Grid Test Model. Further, a steady-state analysis with the inner loop applied over the developed model, which serves as a standard reference case for contingency analysis, is presented.

- **Further Analysis on Steady State Contingency Analysis** : This chapter describes further considerations for the contingency analysis conducted on the CIGRE DC Grid Test Model.

- **Conclusions and Future Work** : This chapter summarises conclusions obtained from the thesis work. Further, some suggestions for future research in this topic are introduced.

2

About VSC-HVDC Systems and MTDC Grids

This chapter describes the MTDC grid topologies that are envisaged to be built using existing AC grids as substrates. A brief introduction into VSC based HVDC configuration and types of DC links applied is given as well. Lastly, motivations to develop a DC/DC converter from a control perspective are presented.

2.1 Introduction

From a transmission perspective, the advantages offered by AC over DC become limited with the increase in the length of the transmission line. As the load demand increases, the losses further increase making AC technology unsuitable for long distance transmission. Further, the foreseen grid integration of RES based large MW power plants will adversely affect the AC Grid stability [20]. So far, the existing grid developed is using AC technology, but is now envisaged to have a DC grid which will be developed over the AC grid as a substrate. This DC grid can be further perceived as an extension of the AC grid and will be developed to enable efficient transmission of large amounts of power over long distances.

The HVDC Links installed and in operation till now, in majority of the cases, have been point-to-point configurations with very few exceptional cases as [26]. Since MTDC grids are yet to be developed, the topology of the same is still a subject of research. The development of DC/DC converters including its control strategies and its function in MTDC grid needs to be further investigated as well.

2.2 DC Grid over existing AC Grid substrates

In order to develop a MTDC grid using the existing AC grid as a substrate, much decision and planning of the expansion of the HVDC Links depends upon the load demands which can be of varying nature. Hence, developing a prior smaller network of HVDC links into a DC network requires considerable planning which would take into account the varying load demands over the AC side and optimisation of AC generation as well[20]. Further, integration of these smaller DC networks into a MTDC grid will require grid planning considering physical assets. These physical assets could include cross-country HVDC links or a part of them. The control structure of the HVDC grids could also be cross-country, with one geographical location

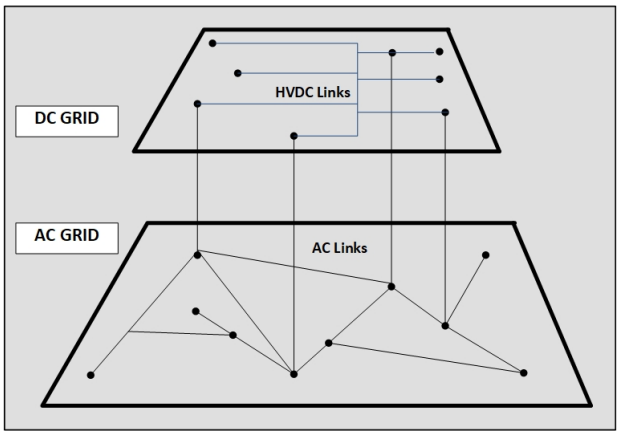

Figure 2.1: DC Grid as a Substrate over the AC Grid [20].

controlling the power while the other controlling the voltage, with both stations being in different countries [21]. Hence, given the varying load demand, proper utilisation and control of these DC links will involve many different principles and would require development of new DC Grid codes as well.

Considering the mentioned scenarios and the role of a DC/DC converter in successfully integrating smaller DC networks into a MTDC grid, maintaining acceptable voltage level and current direction will be the foremost priority from a technical perspective. Further, as shown in Figure 2.1, the typical MTDC grid topology developed should be able to handle the (n-1) DC link contingency i.e the MTDC grid should not become unstable when one of the DC links is disconnected. This would require the VSC to be sufficiently rated along with provisions for bi-directional power flow. Correspondingly, it would be required that the DC Links be rated sufficiently in order to handle the greater share of current flow, following a (n-1) contingency. Furthermore, to provide power security, there should be provisions made in grid planning concerning scenarios where loss of power in one DC link could be re-routed though the existing AC grid, in order to maintain stability in both AC & DC grids [22].

2.3 VSC based HVDC Systems

In this section, an introduction to a VSC based HVDC System is provided. The schematic shown in Figure 2.2 is a typical two-terminal VSC-HVDC system. The AC bus at both ends are connected to transformers which are provided with tap-changers that can step up/down voltage levels. These converter transformers are used to eliminate third-order harmonics and their multiples along with providing galvanic isolation to the VSCs. The High Frequency (HF) Filters are used to filter the high order harmonics [23].The control strategy maintained is that the VSC at the sending end is set for a stiff DC voltage, while on the receiving end, the other VSC provides power control by generating a 3-phase alternating voltage of desired phase, magnitude and frequency.

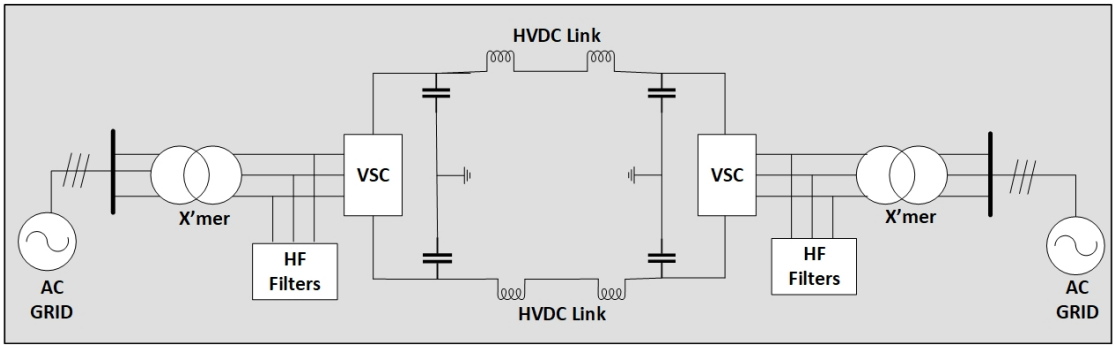

Figure 2.2: VSC based HVDC System [7].

The VSCs have the ability to generate an alternating voltage such that independent control of active and reactive power can be made possible. Moreover, the semiconductor valves (thyristors, IGBTS ect.) used in VSCs allow bi-directional flow of current. Hence, the power flow can be reversed without the need to reverse the voltage polarity. This control flexibility offered by the VSC based HVDC links makes them very suitable to be integrated into a MTDC grid network. The control structure of a VSC can be further used in active and reactive power flow control. The modulation technique used for the semiconductor valves can be either Pulse Width Modulation (PWM) or Space Vector Modulation (SVM).

2.4 Types of HVDC Links

A point-to-point VSC based HVDC configuration can have many configurations of DC links. In this thesis, the CIGRE DC Grid Test Model is used which consists of monopole and bipole DC links. An introduction to the same is given in the sections below. (Explaining other types of DC links is out of scope with the thesis.)

2.4.1 Monopole DC Link

As shown in Figure 2.3, a Monopole HVDC link has one conductor and utilises earth or sea as the return path. The DC link usually operates with negative polarity with respect to ground. Monopole HVDC links are used only for low power rating and mainly for cable transmission, not for overhead lines. Monopole DC links can be converted into bipolar DC links by applying additional substation pole and a transmission pole [23].

2.4.2 Bipole DC Link

As shown in Figure 2.4, a Bipole DC Link has two conductors: one operating with positive polarity and the other with negative polarity. There are two VSCs con-

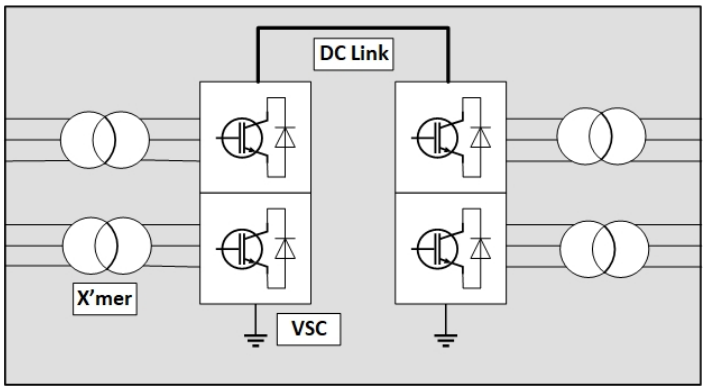

Figure 2.3: Monopole DC Link[23].

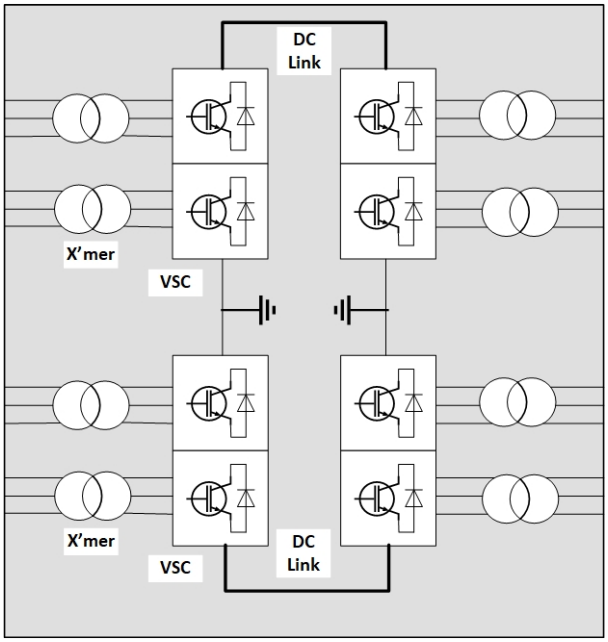

Figure 2.4: Bipole DC Link [23].

nected in series at each ends of the DC link. The neutral point, i.e., the junction between the VSCs may be grounded at one end or at both the ends, as required. If the neutral point is grounded at both ends, then each pole can be operated independently. This type of DC link is used for overhead long distance HVDC transmission systems and for back-to-back HVDC configurations as well [23].

2.5 Network Topologies for MTDC Grids

As no MTDC grids is yet in operation, only theoretical topologies are reported in literature, each of them offering advantages and disadvantages based on their configuration. The simplest MTDC grid can be a straightforward cascaded HVDC links topology, wherein all the HVDC Links are connected in a point-to-point configura-

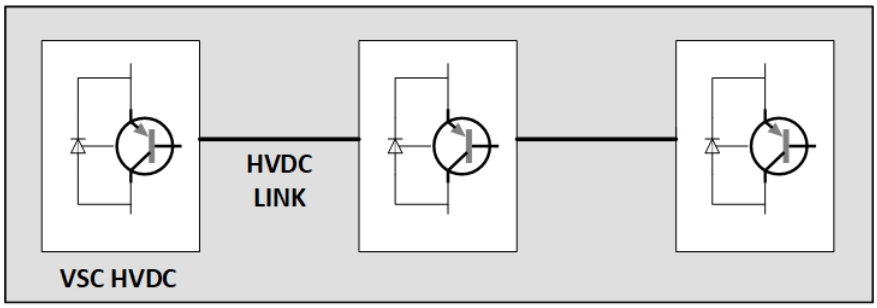

Figure 2.5: Radial DC System [24].

tion. In such a Radial MTDC grid, there are no meshes or redundancy on the DC side. However, such a Radial topology MTDC grid is not a grid per-se, but can be implemented as an alternative or a bypass to AC Lines, or even as a connection between two asynchronous AC grids. Another topology can be that of a meshed DC system, with a number of connections between the AC and DC system. Such a system will offer redundancy on the DC side, however the number of VSCs per DC links could be more if power needs to be controlled on every DC link [22].

In this thesis, the modelling for the DC side will developed on the CIGRE DC Grid Test Model, which consist of a radial and a meshed topology for MTDC grids. Hence, a brief introduction of these two topologies is presented. It should be noted that many such topologies are reported to be developed theoretically, such as - STAR topology with multiple point-to-point DC links, STAR topology with central DC link etc.

2.5.1 Radial Topology

A Radial Topology is the simplest topology of the of a DC Grid, where there is only one path to any converter. As shown in Figure 2.5, this topology of MTDC grid can be implemented with many DC links in a cascaded configuration. In case of contingencies on any of the DC link, the faulty DC link can be isolated and power exchange between healthy DC links can still be operational. The DC grid will still maintain stability, provided that the VSCs are operational [24].

2.5.2 Radial Topology in Star Configuration

A Radial Topology in Star Configuration, as shown in Figure 2.6, can be constructed to maintain power-exchange between DC links of different voltage levels. However, any fault on the DC/DC converter would interrupt the power exchange over the entire MTDC grid structure. Due to this, reliability of this topology is low and is likely that DC grids in the future will not be constructed in this fashion. This issue can be further mitigated by using a double-bus system but would increase costs. [24]. However, the importance of implementing a DC/DC converter can be seen in this topology.

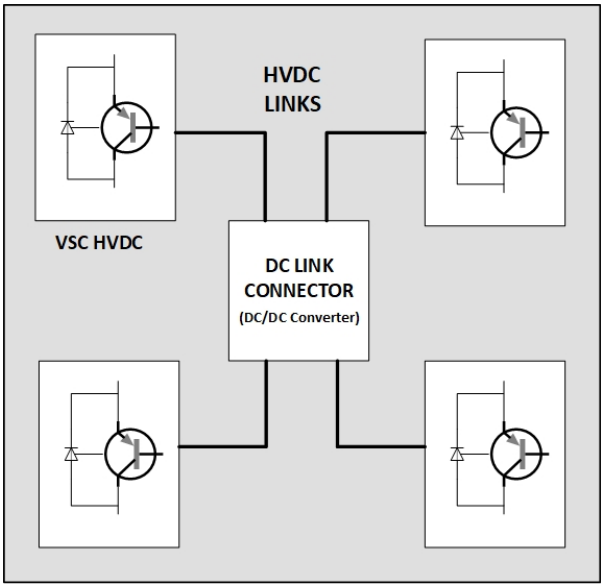

Figure 2.6: Radial DC System in Star Configuration [24].

2.5.3 Meshed Topology

A meshed DC grid topology offers more than one route for power-exchange between two VSCs. In case of a contingency on any one of the DC links, the faulty DC link can be removed from the system, without interrupting the power exchange between the converters, while maintaining the grid stability. However, due to loss of the DC link, the DC power flow might be restricted in the remaining of the cable/overhead lines.

It should be mentioned that the reliability of the a meshed DC Grid is higher than a radial and a star-connected topology. A meshed DC grid topology can survive in some circumstances of (n-2) contingencies, with limited power transfer [24].

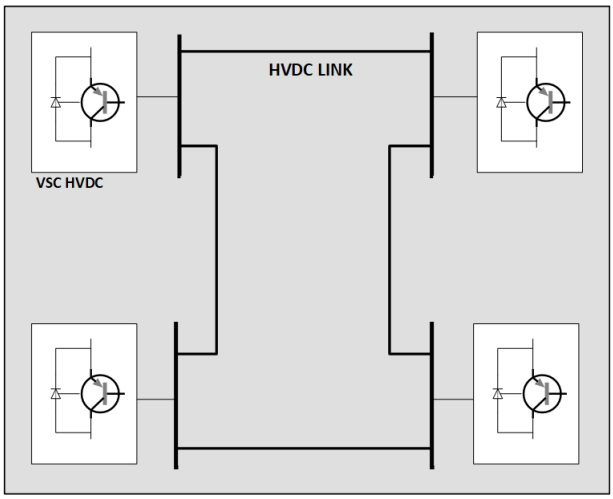

Figure 2.7: Meshed DC Grid [24].

2.6 Motivations for developing a DC/DC Converter

As previously explained, in a classical VSC based HVDC point-to-point configuration, the DC link between two VSC is used to facilitate DC power flow, with one VSC controlling the DC link voltage, while the other VSC for power control. However, MTDC grids are expected to evolve from the interconnection of HVDC systems of different voltage ratings. In such a DC grid, the voltage ratings, converter ratings and the types of DC links will be different. The operating strategy will also be different considering the varying load demands on the AC side.

Correspondingly, interconnecting systems of different voltage levels and to facilitate power flow over the DC Grid, a DC/DC converter might be an alternative solution to this requirement. In a meshed MTDC grid, power control can only be achieved only when the number of DC links are less than the number of installed converters, as argued in [25]. For every n converters present, only n-1 DC links can be be controlled for power flow. The presence of a DC/DC converter can assist in regulating the loading of specific limits and maintaining the DC bus voltages. Furthermore, the device can be used for preventing overloading of the DC links in case of contingencies, disconnection of faulty links, while maintaining power flow in healthy parts of the DC grid [24].

Moreover, a list of complete functions of a DC/DC converter that can be *series embedded* in an MTDC grids are presented below:

- Establish common DC voltage over a meshed system.

- DC Power flow regulation.

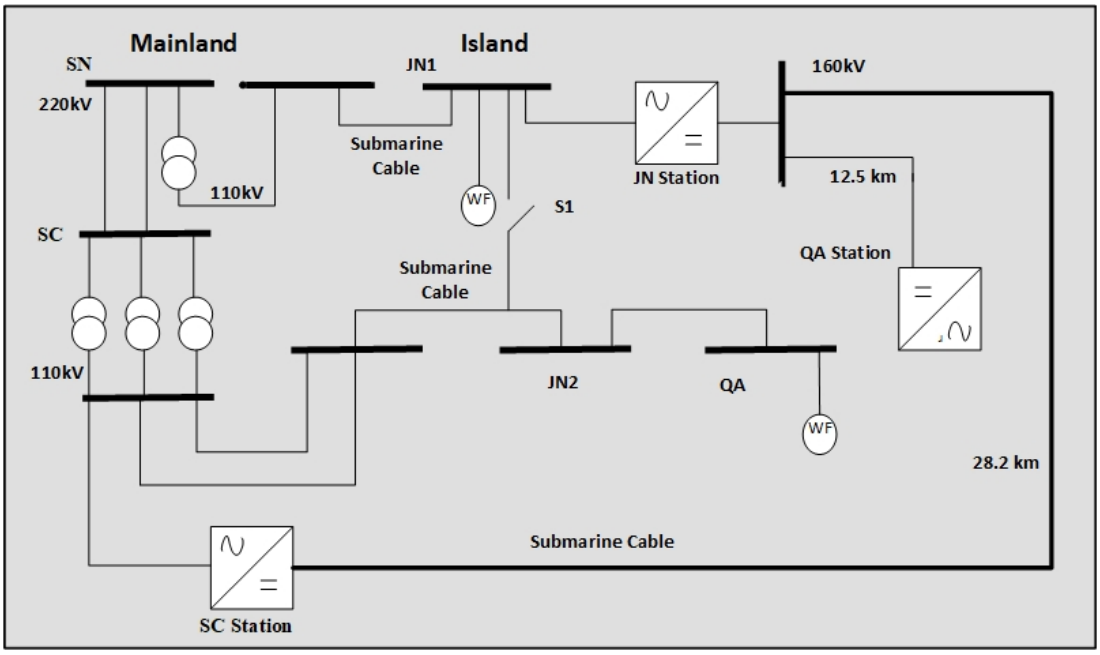

Figure 2.8: Network Configuration for Nanoa 3 Terminal VSC-HVDC [26].

- Current flow regulation and direction.
- DC bus voltage control.
- Reduce losses that can help utilise conductor ratings better.
- Elimination of the intermediate AC interconnection will reduce the number of conversion stages required, thereby lesser equipment will be needed.

A DC/DC converter might not be required in case the MTDC grid has the capability of redistributing the power through an AC network. Further, in some cases, the DC link can be used as a back-up or a bypass for AC power instead. Such a case study is discussed in the next section.

2.7 VSC HVDC based three-terminal project in Nanoa Island in China

In order to meet the renewable energy generation targets and to supply to the increasing load demand, many RES based power plants are being developed in China. China recently commissioned a pioneering +/- 160kV three-terminal HVDC link in Nanoa Island located at the west coast. As shown in Figure 2.9, a three terminal VSC based HVDC system project is built at Shantou, Nanoa Isand in China by the local network operator *China Southen Power Grid* in order to deliver power

produced by Wind Farms (WF) to the mainland consumers.

The network configuration is designed to deliver power to the Mainland from the generation centres at JNI and JN2. For the JN1 terminal, the power is delivered to the Mainland through a step-up transformer. For the JN2 terminal, the power is delivered to the Mainland using a step-up transformer and through a cascaded network of AC buses with a bypass switch. The DC link implemented between the JN Station and SC station is used as a bypass for the AC system to deliver power to the Mainland. In case of AC contingencies at the JN1 station, the power can be redistributed through the DC link and be delivered to the Mainland through the SC station and the step-up transformers.

The SC converter station is designed with a capacity of 2000 MVA and is located at the mainland to generate power through WF. These are connected to buses SN (84 MW) and JN1 (45 MW) export power at 220kV to the SN station. Both AC and DC transmission cables are employed between the Island and the Mainland, thereby maintaining two transmission corridors to accommodate power transfer at both, SN & JN1 locations. To facilitate the same, the CB between JN1 & JN2 is open under normal operating conditions.

Each converter station consist of an AC circuit breaker, converter transformer, pre-charge resistor, bypass switch, DC disconnect and Modular Multilevel Converter (MMC). The DC network consist of submarine cables, overhead lines (OHL) and underground cables. The developed system has a flexible operation mode to handle different scenarios of network connections. The operation mode consist of -

- Parallel operation of AC and DC lines
- Only DC operation
- STATCOM operation

The control system of this 3-terminal structure consist of four components -

- SCADA for system sequence control, data monitoring and acquisition.
- SCS (system co-ordinate control) to manage power flow between AC and DC network.
- Master-Slave control is applied for co-ordination between each converter station.

- Station Online Recommissioning using specific DC breakers so that the entire system does not require a shut down in case of maintains of a sub-ordinate station.

For complete explanation of the control system and for further understanding about the network, the reader is referred to [26].

3

DC Side Model of CIGRE DC Test Grid

This chapter describes the CIGRE DC Grid Test Model developed by Work Groups B4-57 and B4-58. Its implementation for studying DC power flow is described. The averaged model of the series embedded DC/DC converters developed is explained as well. Further, a steady state analysis of DC power flow on the developed model is presented.

3.1 Introduction

HVDC technology developed till now has been mainly used for point-to-point transmission system, with usually the sending end controlling the voltage and the receiving end controlling the power flow [7]. However, with the development of the Nanoa 3-terminal HVDC grid in China, as explained in Section 2.7 of Chapter 2, developing an integrated network of HVDC links into an MTDC grid is forseen. Further, to control power flow over the MTDC grid it is understood that current over (n-1) DC links can be controlled by utilising not less than n converters [28]. In other words, in order to control DC current flow, the number of converters should be atleast one more than the total number of DC links in an MTDC system. Moreover, to maintain current levels and voltage control over the MTDC grid, a *DC Power Flow Controller* device i.e. DC/DC converters must be series embedded into the MTDC grid. This DC/DC converter is expected to perform a variety of functions in the DC Grid.

Correspondingly, the Transmission Grid Operators (TSO), academic community and manufacturing companies have shown a strong interests in developing meshed HVDC grids with series embedded DC/DC converters in the future. The vision of creating a such a MTDC grid network is quite futuristic and is yet subject to basic research. As mentioned in Section 1.2 of Chapter 1, much research regarding DC/DC converter topologies, VSC based control strategies involving AC and DC side has been published, but understanding DC power flow independent of the AC side along with the role of DC/DC converter from a control perspective over the MTDC grid, is yet to be investigated and understood.

In order to develop a common research platform, CIGRE's work groups B4.57 and B4.58 have developed a DC Grid Test System as a benchmark model. This bench-

mark model has been evolved from being a radial HVDC grid initially to a meshed grid with series embedded DC/DC converters.

For complete information about the benchmark model, the reader is referred to [27]. The DC side modelling is conducted in PSCAD and is referenced from the same.

3.2 Description of the DC Grid Test System

The CIGRE benchmark model intends to include all types of AC sources (Wind Farms) and Loads (Oil & Gas Platforms and other loads) over which a MTDC grid can be built, using AC grid as substrate. The complete model is as shown in Figure 3.1. This includes 2 onshore AC systems, 4 offshore AC systems, 2 DC nodes and 3 VSC-HVDC systems. The DC side configuration is differentiated into three subsystems - DCS 1, DCS 2 and DCS 3. Further, the system consist of two DC voltages - +/- 400kV & +/- 200kV. The abbreviations used for denoting equipment in the benchmark model are given in Table 3.1.

The DCS 1 subsystem is a two-terminal symmetrical monopole HVDC link rated at +/- 200kV and connects an offshore wind power plant at terminal C1 to onshore node at A1.

The DCS 2 subsystem is a four-terminal radial HVDC configuration with symmetrical monopole cables rated at +/- 200kV. The network connects offshore wind power plant at F1, the offshore oil & gas platform at E1 and the onshore node at B3. This network is further extended to the inland load centre at B2. This system also includes a DC/DC converter.

The DCS 3 subsystem is a five-terminal meshed HVDC configuration that includes both, bipole and symmetrical monopole cables and includes a DC/DC converter.

Further, there is no direct connection between any DCS 1 and DCS 2, however DCS 1 and DCS 3 are interconnected through an AC link. Since the objective of the thesis is to conduct steady state analysis for DC power flow only, the DCS 1 subsystem is *DC decoupled* from the other subsystems.

To further detail the notations, the description is given in Table 3.1 must be read in conjunction with Figure 3.1.

3.3 DC Side Equivalent Model in PSCAD

Since the aim of the thesis is to perform steady analysis with focus on the DC side, the VSCs are modelled as voltage controlled DC sources. The VSCs that are in voltage control mode are modelled as stiff voltage sources, while the VSCs that are

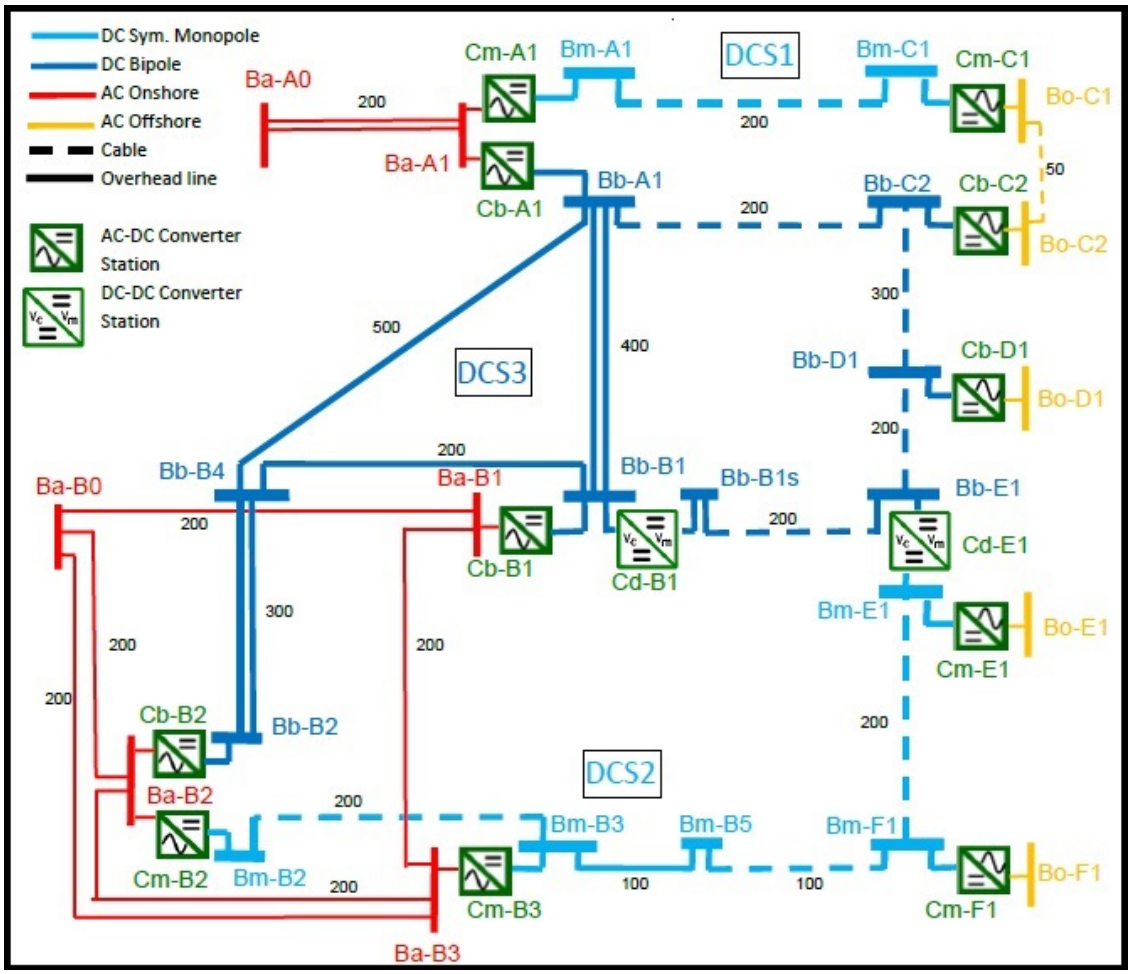

Figure 3.1: DC Grid Test Model from CIGRE [26].

Table 3.1: Equipment Abbreviation. [27].

Type	**Abbreviation**
Onshore AC Bus	Ba
Offshore AC Bus	Bo
Symmetrical Monopole DC Bus	Bm
Bipole DC Bus	Bb
Monopole AC-DC Converter	Cm
Bipole AC-DC Converter	Cb
DC/DC Converter	Cd

Table 3.2: Converters connected to DC buses. [27].

Sr. No	DC Bus	Subsystem	Converter	Voltage (kV)	Rated Power (MW)
1	BmA1	DCS 1	CmA1	200.00	NA
2	BmC1	DCS 1	CmC1	200.00	+ 391.5
3	BmE1	DCS 2	CmE1	200.00	- 100.5
4	BmF1	DCS 2	CmF1	200.00	+ 496.88
5	BmB5	DCS 2	None	200.00	NA
6	BmB3	DCS 2	CmB3	200.00	- 800
7	BmB2	DCS 2	CmB2	200.00	NA
8	BbE1	DCS 2	CdE1	400.00	NA
9	BbC2	DCS 3	CbB2	400.00	+ 600
10	BbD1	DCS 3	CbD1	400.00	+ 993.75
11	BbB2	DCS 3	CbB2	400.00	- 1700
12	BbB4	DCS 3	None	400.00	NA
13	BbB1	DCS 3	CbB1	400.00	- 1500
14	BbB1s	DCS 3	CdB1	400.00	NA
15	BbA1	DCS 3	CbA1	400.00	NA

in power controlled mode are modelled as voltage controlled sources that can adjust their output voltage such that a certain desired power is obtained. Table 3.2 shows ratings and power set-point of the converters and details of the DC busses with their power input/output into the MTDC grid. In total, there are 15 AC/DC converters out of which 8 are in power control mode, 3 are in voltage control mode, while the rest 4 are used for linking DC buses and DC/DC converters. The VSC losses are not of importance and are neglected here.

It should be noted that the current flow convention is taken from the *Source* to the *Load*. Hence power being injected into the grid has a positive sign, while load is shown with a negative sign. This convention is maintained throughout the steady state analysis.

(The section A.1 of Appendix 1 shows power controlled DC bus implementation in PSCAD.)

3.3.1 Averaged Model for the DC/DC Converter

To model the DC/DC converter for DC load flow studies, an averaged model for the DC/DC converter from [25] is considered. As shown in the Figure 3.2, the model consist of a controllable voltage source behind an inductance on the input side and a controllable current source behind a capacitance on the output side. The DC sides are linked through the power balance principle expressed as -

$$V_1.I_1 = V_2.I_2 \tag{3.1}$$

In the averaged model of the DC/DC converter, the controlled variables V_{a_1} and I_{a_2} provide inputs to the voltage and current sources. The control variable V_{a_1} for

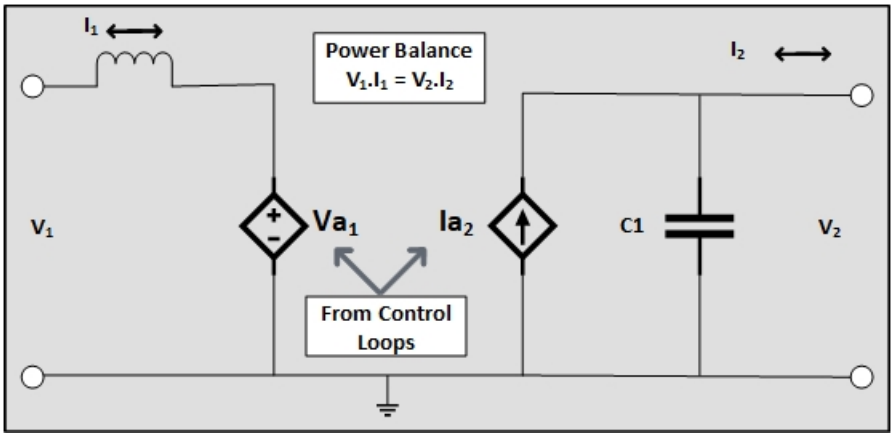

Figure 3.2: Averaged Model of a DC/DC converter. [25].

voltage on one side of the DC/DC converter is provided as an input signal to control variable I_{a_2} for current control on the other side of the DC/DC converter, through the use of power balance equations. In this way, voltage and current can be balanced over both the sides of the DC/DC converter using varying inputs from the controlled variables and through the use of power-balance equation. The control signals to these controlled variables are provided by the control loops developed which are further explained in Chapter 4 of this report. Since this study is specifically about DC Load Flow studies, harmonics and AC side faults are not considered neglected.

Section A.2 of Appendix 1 shows the averaged DC/DC converter model.

3.3.2 DC Link Resistances

Equivalent resistances of all the cables and Overhead Lines (OHL) are presented in Table 3.3 where the per unit length resistance is provided along with the length of of the cable/OHL. It should be noted that this data is obtained from [27]. Since only steady state analysis is performed the inductance and capacitance parameters of the cable/OHL are not part of the model. Further, the AC links that indirectly connect the DC systems are also not considered.

3.4 Steady State Analysis

The modelled DC system in this thesis is to be used for DC power flow analysis and to test the control strategies developed for current and voltage control of the DC/DC converters. Under normal operating conditions, data from the MTDC grid is obtained to be further used a reference case for comparison with the test cases run in the thesis. This includes the DC bus voltages, DC link currents and the voltages over the DC/DC converters. Further, under normal operating conditions the current

Table 3.3: Equivalent Resistances of HVDC Links.

Sr No.	From	To	Subsystem	R (ohm/km)	Length	Total
1	BmA1	BmC1	DCS 1	0.011	200	2.2
2	BmE1	BmF1	DCS 2	0.011	200	2.2
3	BmF1	BmB5	DCS 2	0.011	100	1.1
4	BmB5	BmB3	DCS 2	0.0133	100	1.33
5	BmB3	BmB2	DCS 2	0.011	200	2.2
6	BbA1	BbC2	DCS 3	0.011	200	2.2
7	BbC2	BbD1	DCS 3	0.011	300	3.3
8	BbD1	BbE1	DCS 3	0.011	200	2.2
9	BbE1	BbB1s	DCS 3	0.011	200	2.2
10	BbB1	BbB4	DCS 3	0.0114	200	2.28
11	BbA1	BbB1	DCS 3	0.0114	400	4.56
12	BbA1	BbB4	DCS 3	0.0114	500	5.7
13	BbB2	BbB4	DCS 3	0.0114	300	3.42

flow values through the DC/DC converters obtained are assumed as set-points in the simulated test cases. Given, the measured voltage and current set-points, power flow set-points over the DC/DC converter are obtained as well.

Initially, the DC/DC converters are assumed as uncontrolled devices and simulations are run to obtain initial DC power flow values in the modelled DC grid. These are modelled as AC transformers with instant transformer ratios. For DC/DC 1 converter, the transformation ratio is 1:1, while for DC/DC 2 transformer, the ratio is 1:2 as it connects DCS 2 subsystem to DCS 3 subsystem with a voltage difference from 200kV to 400kV.
Table 3.4 shows that in this reference case, all the 15 DC busses present in the modelled DC grid are maintained within a permissible range of 0.95-1.05 p.u.

Table 3.5 details that 2 out of 13 DC links are over-loaded. It should be observed here that the CIGRE DC Grid Test Model is not an ideal model, hence its plausible that some of the DC links be overloaded in this case.

Figure 3.3 shows the load flow results for the reference case in the CIGRE DC Test Grid Model. The details of the modelled DC Grid are successfully adapted from the CIGRE DC Test Grid model.

Section A.3 of Appendix 1 shows the implementation of the DC grid model in PSCAD.

Table 3.4: DC bus voltages under steady state conditions.

Sr No.	**Bus**	**Actual kV**	**Base kV**	**p.u**	**Control**	**System**
1	BmA1	200.00	200.00	1.00	Voltage	DCS 1
2	BmC1	204.22	200.00	1.02	Power	DCS 1
3	BbE1	399.04	400.00	1.00	NA	DCS 2
4	BmE1	199.52	200.00	1.00	Power	DCS 2
5	BmF1	199.82	200.00	1.00	Power	DCS 2
6	BmB5	197.23	200.00	0.99	NA	DCS 2
7	BmB3	194.10	200.00	0.97	Power	DCS 2
8	BmB2	198.00	200.00	0.99	Voltage	DCS 2
9	BbC2	405.03	400.00	1.01	Power	DCS 3
10	BbD1	404.68	400.00	1.01	Power	DCS 3
11	BbB2	388.00	400.00	0.97	Power	DCS 3
12	BbB4	388.89	400.00	0.97	NA	DCS 3
13	BbB1	393.81	400.00	0.98	NA	DCS 3
14	BbB1s	393.82	400.00	0.98	NA	DCS 3
15	BBA1	402.00	400.00	1.01	Voltage	DCS 3

Table 3.5: DC link current under Steady State conditions.

Sr No.	From	To	System	Rated kA	Actual kA	% Load
1	BmA1	BmC1	DCS 1	1.962	1.930	0.984
2	BmE1	BmF1	DCS 2	1.962	0.135	0.069
3	BmF1	BmB5	DCS 2	1.962	2.350	1.198
4	BmB5	BmB3	DCS 2	3.000	2.350	0.783
5	BmB3	BmB2	DCS 2	1.962	1.770	0.902
6	BbA1	BbC2	DCS 3	2.265	1.370	0.605
7	BbC2	BbD1	DCS 3	2.265	0.105	0.046
8	BbD1	BbE1	DCS 3	2.265	2.560	1.130
9	BbE1	BbB1s	DCS 3	2.265	2.370	1.046
10	BbB1	BbB4	DCS 3	3.500	2.150	0.614
11	BbA1	BbB1	DCS 3	3.500	1.795	0.513
12	BbA1	BbB4	DCS 3	3.500	2.290	0.654
13	BbB2	BbB4	DCS 3	3.500	2.220	0.634

Table 3.6: Set-Points for DC/DC converters under steady-state conditions.

Sr No.	**Equipment**	**Current (kA)**		**Voltage (kV)**		**Power (MW)**
		Input	Output	Input	Output	
1	DC/DC 1	2.377	2.377	393.82	393.05	936.1
2	DC/DC 2	0.185	0.35	399.04	199.52	73.82

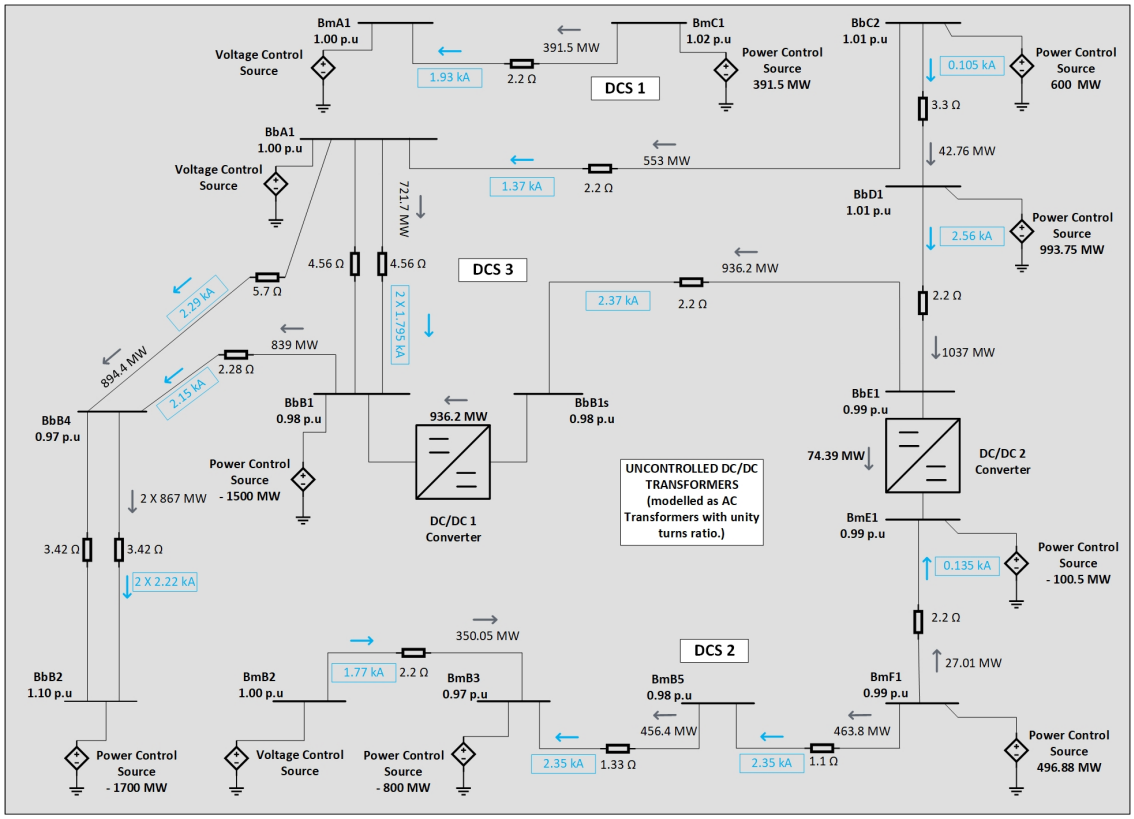

Figure 3.3: DC Grid Model in PSCAD

4

Control Loops Developed

This chapter describes the Inner and Outer control loops developed for DC power flow and their implementation over the developed DC side model of the CIGRE DC Grid Test Model

4.1 Introduction

As described in the preceding chapter, to understand DC load flow in steady state MTDC grid, a steady state model of CIGRE DC Grid Test Model is developed with only the DC side. As per the benchmark model shown in Figure 3.1, there 15 DC buses with 8 DC buses for power control, 3 DC buses for voltage control, 2 buses interconnected between 2 DC/DC converters and remaining 2 DC buses connecting DC links. Further, the model has 13 DC links distributed over 3 subsystems - DCS 1, DCS 2 and DCS 3. Furthermore, by using arbitrary AC transformers to emulate DC/DC converters as uncontrolled devices, power set-points for both the DC/DC converters are obtained as shown in Table 3.6. The DC bus voltages and DC link currents are observed to be within permissible limits.

To investigate the DC load flow and to verify the designed control strategies on the DC/DC converters for current and voltage control, (n-1) contingencies are simulated on the developed model. In other words, the behaviour of DC power flow in the developed test system is investigated by disconnecting each of the 13 DC links, one-by-one. Further, it is to be studied which DC links when disconnected will cause the entire DC Grid to become unstable.

With the averaged model of the DC/DC converter in place, inner loops for current control and outer loop for voltage control are created using Proportional Integral (PI) controllers, as explained further in this Chapter. To introduce the reader to the PI controller, a short description of the principle involved is explained in the next section. Further, control principles involved in DC power flow and their analogous nature to AC power systems is explained as well.

4.2 Control Principles in MTDC grids

The control of DC voltage and current in an MTDC grid can be considered analogous to frequency control in an AC Grid, as can be seen in Figure 4.1. The primary response control principles in an MTDC grid are similar to that of an AC Grid.

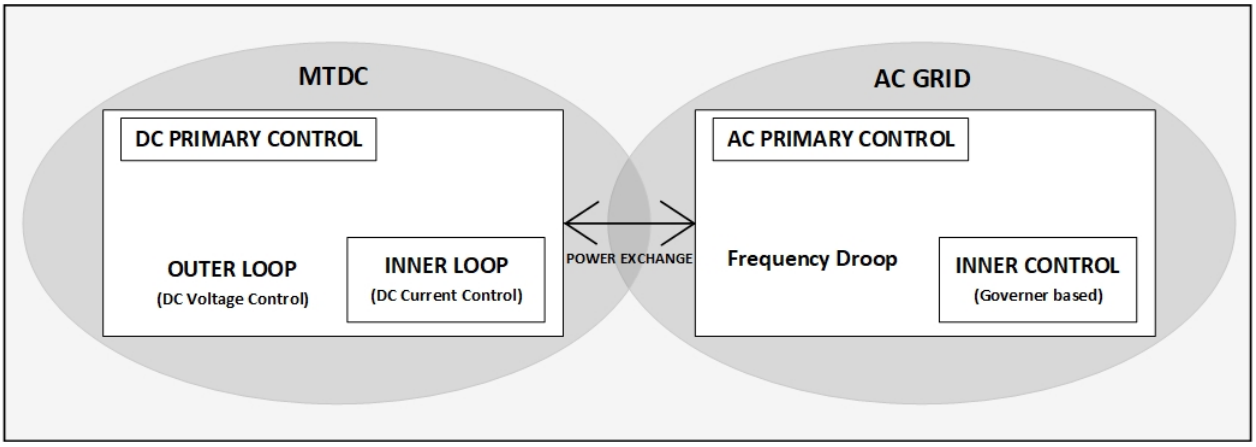

Figure 4.1: Primary Response Control Structure of AC Grid and MTDC

In an AC grid, whenever there is an unbalance in load over the transmission lines, the frequency of the system will increase or decrease prompting action from the generators to balance power generation [29]. This primary control action will help maintain power-balance in the system and make sure that the AC grid achieves stability. Analogically, in a MTDC grid whenever there is an unbalance in current, the DC bus voltages will increase or decrease prompting action from the DC capacitors and HVDC cable capacitance in discharging or charging. This primary control action will help maintain voltages within the permissible limits in the system and make sure that the DC power is regulated [28].

Correspondingly, in case of a DC grid, if the VSC was exporting power to the AC grid, an outage on the converter will see a surplus in power coming into the DC grid and increase the system DC voltage. Likewise, if the VSC is was importing power into the DC grid, an outage over the converter will see a deficit of power coming into the DC grid and decrease the system DC voltage.

In an AC grid, the frequency is considered to be Global Factor for control. By maintaining frequency, load demand can be balanced with generation capacity. For maintaining AC grid stability, the system frequency has a permissible range (49.9-50.1 Hz) [30].

However, in DC grids the control is much more complicated as the stability in a MTDC grid is governed by many factors like DC voltages, DC current flow, fast dynamics and also the DC voltage is not same at all the nodes in the DC grid. Due to this, a single global factor for governing stability over MTDC grid cannot be developed. Yet, it is envisaged that the DC voltage stability over the DC nodes in MTDC grids is best option for the same [28]. Different control strategies can be applied to control and balance the DC voltage on a MTDC grid, especially in the case of outage over any of the meshed HVDC Links.

In an MTDC grid, theoretically, control of current at all the DC links is achiev-

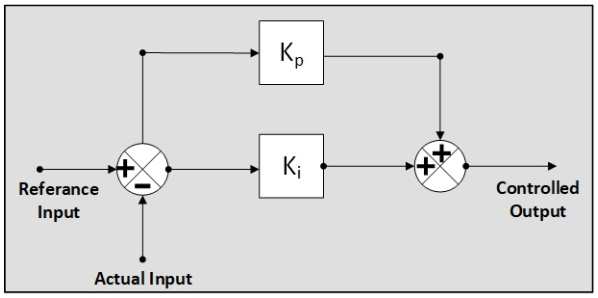

Figure 4.2: PI Controller

able only if the number of VSCs exceed the number of DC links. In other words, for every n number of converters present, current control over the MTDC grid is possible only if there are (n-1) DC links present. If there are equal or more number of DC links than converters present, it would not be possible to regulate DC current and voltage over the MTDC grid. Further, additional control devices could be required in a meshed HVDC network to regulate the DC voltage and current. One of these devices, called DC/DC converters need to be series embedded over the MTDC grid in order to regulate DC power flow, especially in case of DC link outages.

The control strategies developed on the studied DC/DC converters consist of inner and outer loops. The inner loop is utilised for current control, while the outer loop is utilised for voltage control. Besides these schemes, control loops can also be designed for power control and impedance control. These are however not considered in this thesis, as the aim is to develop control schemes for voltage and current control.

4.3 PI Controller

The principle of a (PI) controller as shown in Figure 4.2 is to rectify error between input and a reference signal and generate a corrected signal which would drive the steady-state error to zero. For this purpose, the PI regulator uses a proportional constant and an integrating constant. The role of a proportional constant is to create a proportional signal to the error signal by multiplying it with a constant K_p, while the role of the integrating constant K_i to produce a signal that is time-integral of the input signal [31]. The proportional constant helps to achieve steady state while the integral constant uses area-time integration to drive the steady state error to zero.

The summation output of this is a corrected signal which is given as input to a voltage controlled source over the averaged model of the DC/DC converter, as shown in Figure 3.2 of Chapter 3. The PI controller, to the best of its design limits, will rectify the imbalance between voltage or the current by driving the steady state error to zero, and stabilise the DC Grid following a contingency.

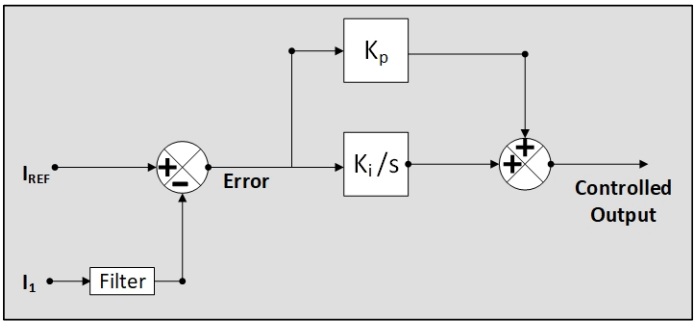

Figure 4.3: Inner Loop for Current Control [25].

4.4 Inner Loop Controller

The inner control loop is developed for controlling the current through one of the sides of the DC/DC converter. In the developed model for DC side, the inner loop is to be applied on both the DC/DC converters that are series embedded in the CIGRE DC Grid Test System.

4.4.1 DC Current Control

The inner loop is developed for current control over the DC/DC converters by using a PI controller. To control the current over the DC/DC converter, the input current I_1 is compared to the required reference current I_{REF}. The output of the regulator is then fed to the V_{a1} terminal of the averaged model of the DC/DC converter as a control signal. In this control loop, the current is controlled on one end through a given set-point. Using power balance, current over the other end will be controlled as well. In effect, the current over the DC Link with the DC/DC converter is controlled.

Figure 4.2 shows an inner loop for current control as described in CIGRE document [25]. The assumed controller parameters are K_i as 0.1s and K_p as 0.1 for both the DC/DC converters. Since an averaged model of the DC/DC converter is used, calculating actual values for control parameters is not motivated. Further, as only DC power flow over the DC Grid is considered while assuming the AC part as ideal, the filters can be neglected.

4.5 Outer Loop Controller

The outer control loop is developed for the DC/DC converter to control the voltage at one of the sides of the DC/DC converter. In the developed model for DC side, the outer loop is to be applied over both the DC/DC converters. The outer loop is designed with two principles - with voltage control and with voltage step ratio control.

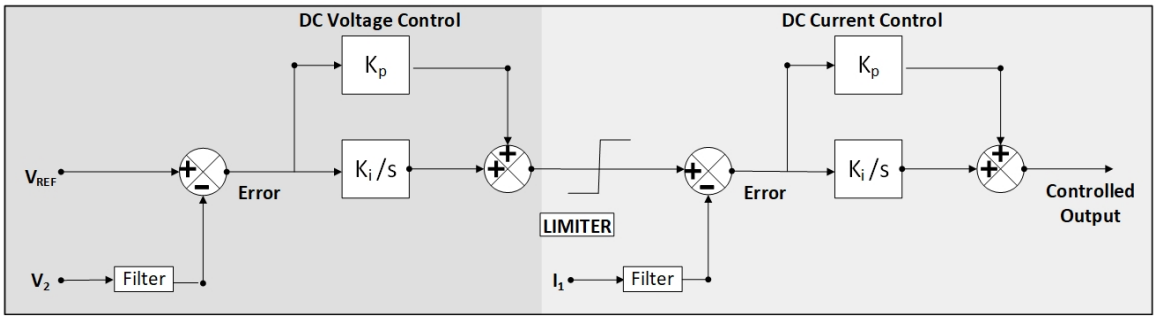

Figure 4.4: Outer Loop for Voltage Control [25].

4.5.1 Voltage Control

The outer loop is developed for voltage control over the DC/DC converters by using a PI controller. To control the voltage over the DC/DC converter, the input voltage V_1 is compared to the required reference voltage V_{REF}. This reference input is set to a predetermined set-point value. The error signal is fed to the PI regulator which, likewise, generates an output that goes to the current controller. The outer loop uses cascaded PI controllers.

Figure 4.4 shows an outer loop for current control as described in CIGRE document [25]. The controller parameters are set as - K_i as 1s and K_p as 0.1 for the outer loop and K_i as 0.001s and K_p as 0.1 for the inner loop. Since an averaged model of the DC/DC converter is used, calculating actual values for control parameters is not motivated. Further, as only DC power flow over the DC Grid is considered while assuming the AC part as ideal, the filters can be neglected.

4.5.2 Voltage Step Ratio Control

In an typical AC transformer, the relationship between the voltage and the windings can be described as,

$$\frac{V_1}{V_2} = \frac{N_1}{N_2}$$

wherein, V_1 and V_2 are the primary and secondary voltages, N_1 and N_2 are number of turns in the primary and secondary windings, respectively [32].

If the ratio of the primary and secondary windings in an AC transformer is *1:1*, the primary and secondary voltages will also correspondingly maintain a ratio of *1:1*. This principle can be applied to controlling voltage in a DC/DC converter.

In this case, as shown in Figure 4.5, the voltage controller will regulate the output DC voltage amplitude equal to the input DC voltage amplitude, using a transformation ratio k_P. The ratio of both the DC voltages is given as an input and is compared with a reference ratio k_{REF}. This reference input is set to a predetermined set-point value depending on whether the DC/DC converter requires voltage to be stepped

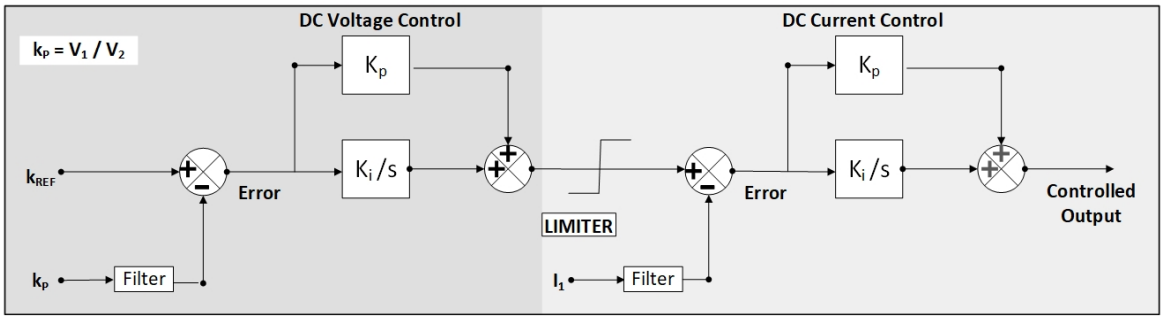

Figure 4.5: Outer Loop for Voltage Control using Voltage Step Ratio Control [25].

up, down or to be maintained the same. The error signal is fed to the PI regulator which, likewise, generates an output that goes to the current controller [25].

This voltage step ratio controller can be implemented in case where two HVDC Links have different voltage ratings and need to be connected in order to create a smaller DC network or expand an MTDC grid. However, this voltage ratio controller can cause cascading voltage dips at DC buses in the MTDC grid, in case the VSC-HVDC system for one such DC Link experiences a voltage dip.

The bandwidth considered K_i as 1s and K_p as 0.1 for the outer loop and K_i as 0.001s and K_p as 0.1 for the inner loop. Since an averaged model of the DC/DC converter is used, calculating actual values for control parameters is not motivated. Further, as only DC power flow over the DC Grid is considered while assuming the AC part as ideal, the filters can be neglected.

Section A.4 and A.5 of Appendix A shows the implementation of the control loops in PSCAD.

4.6 Further on Control Loops

In the thesis, the objective is to design control strategies over series embedded DC/DC converters in MTDC grids, specifically for current and voltage control. Some of the control strategies mentioned in [25] that can be developed are not considered. For completeness, a brief introduction is presented.

4.6.1 Power Control

In this control strategy, the inner loop is designed for current control in the same way as described in section 4.5.1 of this Chapter. The outer loop is designed with a reference power input (instead of a reference voltage) and a measured power input. The error signal is fed to the PI regulator which, likewise, generates an output that goes to the current controller. The outer loop uses cascaded PI controllers.

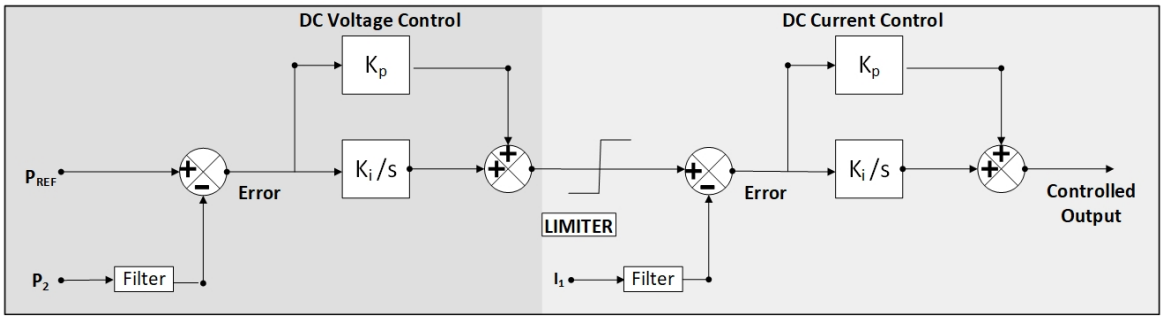

Figure 4.6: Outer Loop for Power Control [25].

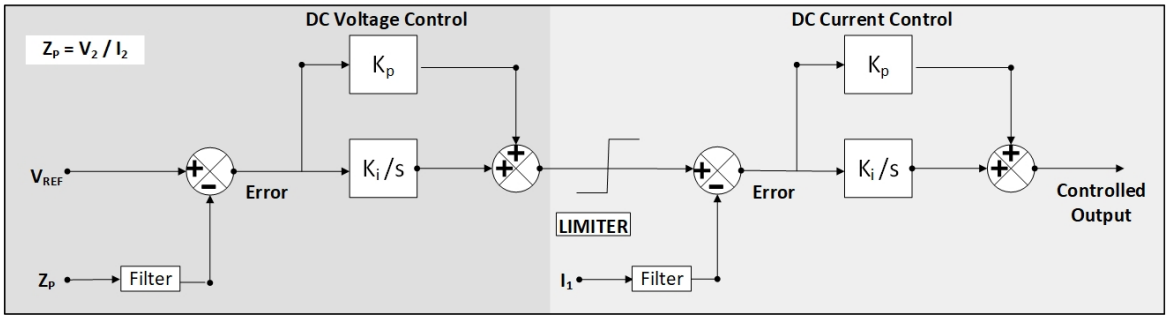

Figure 4.7: Outer Loop for Impedance Control [25].

4.6.2 Impedance Control

In this control strategy, the inner loop is designed for current control, exactly the same way as described in section 4.5.1 of this Chapter. The outer loop is designed with a reference impedance input (instead of a reference voltage) and a measured impedance input. The error signal is fed to the PI regulator which, likewise, generates an output that goes to the current controller. The outer loop uses cascaded PI controllers.

However, with this control strategy, it should be noted that converter on the input side will appear as a DC load with resistance ($V_2/I_2 = constant$), while on the output side the converter will appear as ($V_1/(d^2 * I_1) = constant$, with (d) being the PI controller's corrected output signal. Hence, the resistance on the output side will not be a constant [25].

5

Steady State Contingency Analysis

This chapter presents the results of contingency analysis performed in the developed DC side model of the CIGRE DC Grid Test Model. Further, a steady-state analysis with the inner loop applied over the developed model, which serves as a standard reference case for contingency analysis, is presented.

5.1 Overview

In the following sections, considering the (n-1) contingency criterion, three control strategies are developed and tested for the developed DC side model of the CIGRE DC Grid Test System, with the two series embedded DC/DC series converters. The main function of these control strategies is to regulate current and voltages over the DC grid and achieve steady-state following a disconnection of a DC link.

To test and validate these control strategies, disconnections of each of the 13 DC links is simulated, one-by-one. Initially, contingency analysis over the DC grid is conducted using inner loop for current control. If any of the contingency leads to the DC grid becoming unstable, an outer loop for voltage control is applied to the DC/DC converters to regulate DC bus voltages and maintain DC grid stability.

The considerations assumed for contingency analysis and classification of the DC Links are explained in following sections. However, before introducing the DC link contingencies on the developed model, a reference case is obtained for the sake of comparison of the steady state values. A steady state analysis of the modelled DC grid is given with the series embedded DC/DC converters applied only with inner loop for current control. Figure 5.1 shows the resulting power flow over the DC grid in steady state.

5.2 Steady State Analysis with Inner Loop applied

The set-points for current and voltages over both the DC/DC converters are obtained from Table 3.6 of Chapter 3. The power flow obtained is exactly the same for every DC link, as can be seen when Figure 5.1 is compared with Figure 3.3 of

Table 5.1: DC bus voltages with inner loop on both DC/DC converters.

Sr.No	Bus	P.U Value	Within Tolerance
1	BmA1	1.000	Yes
2	BmC1	1.021	Yes
3	BbC2	0.996	Yes
4	BbD1	0.990	Yes
5	BbE1	1.006	Yes
6	BmE1	1.006	Yes
7	BmF1	0.996	Yes
8	BmB5	1.005	Yes
9	BmB3	1.016	Yes
10	BmB2	0.990	Yes
11	BbB2	1.050	Yes
12	BbB4	1.033	Yes
13	BbB1	1.021	Yes
14	BbB1s	1.023	Yes
15	BbA1	1.000	Yes

Chapter 3. Further, all the DC bus voltages are within the permissible limits, as shown in Table 5.1. Furthermore, as can be seen in Table 5.2, the two DC links in DCS 2 subsystem are overloaded, as expected.

In the next sections, contingencies over all the three subsystems - DCS 1, DCS 2 and DCS 3 are conducted. Each one of the 13 DC links is subjected to a disconnection. DC bus voltages and DC link currents are observed. Further, DC power flow over both the DC/DC converters is observed and grid stability is studied as well.

5.3 Considerations for the Contingency Analysis

The following are the steps and considerations in which contingencies are created over the modelled DC Grid.

- Initially, the DC/DC converters are controlled by only applying an inner loop for current control. A disconnection is made on every DC link for studying (n-1) contingency criterion.

- Current, Voltage and Power variations are observed on every DC link. The changes in current, voltage and power over both DC/DC converters are observed as well.

- If the grid system becomes unstable, an outer loop (voltage and/or voltage-

Table 5.2: DC link currents with inner loop on both DC/DC converters.

Sr . No.	DC Link		Rated kA	% Loading	Overloaded
	From	To			
1	BmA1	BmC1	1.91	97.30	Almost
2	BmE1	BmF1	0.133	6.84	No
3	BmF1	BmB5	2.35	119.8	Yes
4	BmB5	BmB3	2.35	78.3	No
5	BmB3	BmB2	1.76	77.7	No
6	BbA1	BbC2	1.375	60.7	No
7	BbC2	BbD1	0.1	4.4	No
8	BbD1	BbE1	2.56	113.2	Yes
9	BbE1	BbB1s	2.37	67.7	No
10	BbB1	BbB4	2.15	65.4	No
11	BbA1	BbB1	1.79	51.1	No
12	BbA1	BbB4	2.29	94.9	Almost
13	BbB2	BbB4	2.29	65.4	No

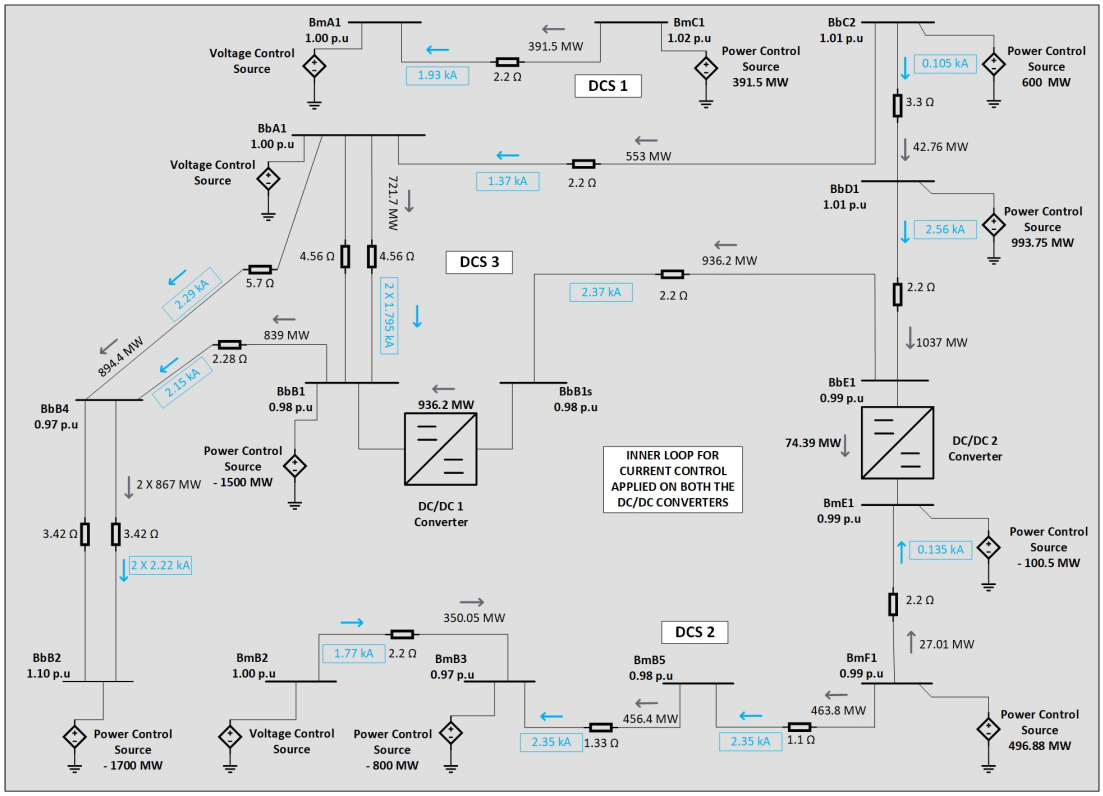

Figure 5.1: Steady State DC Grid Model in PSCAD using Inner Loop

step-ratio) is applied to mitigate the instability. Correspondingly, changes in the current, voltage and power over both DC/DC converters is observed.

- The DC bus voltages are considered acceptable only if they are within 0.95 – 1.05 p.u range (with 400kV as base voltage for DC/DC 1 converter and 200kV base for DC/DC 2 converter.)

- Only overloading of DC links is considered.

With these considerations, the DC links were further classified into two categories as explained in the next section.

5.4 Classification of the DC Links

With only the inner loop for current control applied on both the DC/DC converters, the DC links are classified according to the end result of their disconnections:

- If the grid turns unstable when the DC link when disconnected, the DC link is deemed as a *Critical* DC link.

- If the grid does not turns unstable when the DC Link when disconnected, the DC Link is deemed as a *Non Critical* DC link.

5.5 Contingency Analysis over DCS 1 Subsystem

The DCS 1 subsystem consist of one symmetrical monopole DC link from DC bus BmE1 to BmA1, as can be seen in Figure 3.1 of Chapter 3.

DCS 1 subsystem is electrically connected to DCS 2 subsystem through an AC link (BoC1 to BoC2) and there is no direct DC link connection. Since this analysis is to specifically understand DC power flow over the DC grid and control strategies on the DC/DC converters, the DCS 1 subsystem can be considered to be *DC-Decoupled* from the rest of the subsystems in the DC grid. Hence, when this DC link BmA1 to BmC1 is subjected to a disconnection, there is no power flow deviation that is observed over DCS 2 and DCS 3 subsystems. However, the DCS 1 subsystem does become unstable. The disconnection of this DC link will possibly create an instability on the AC side as well and must be disconnected quickly.

Further, since the disconnection of this DC link does not lead the instability in rest of the subsystems, this contingency is no longer subjected to outer loop control for voltage or voltage step ratio.

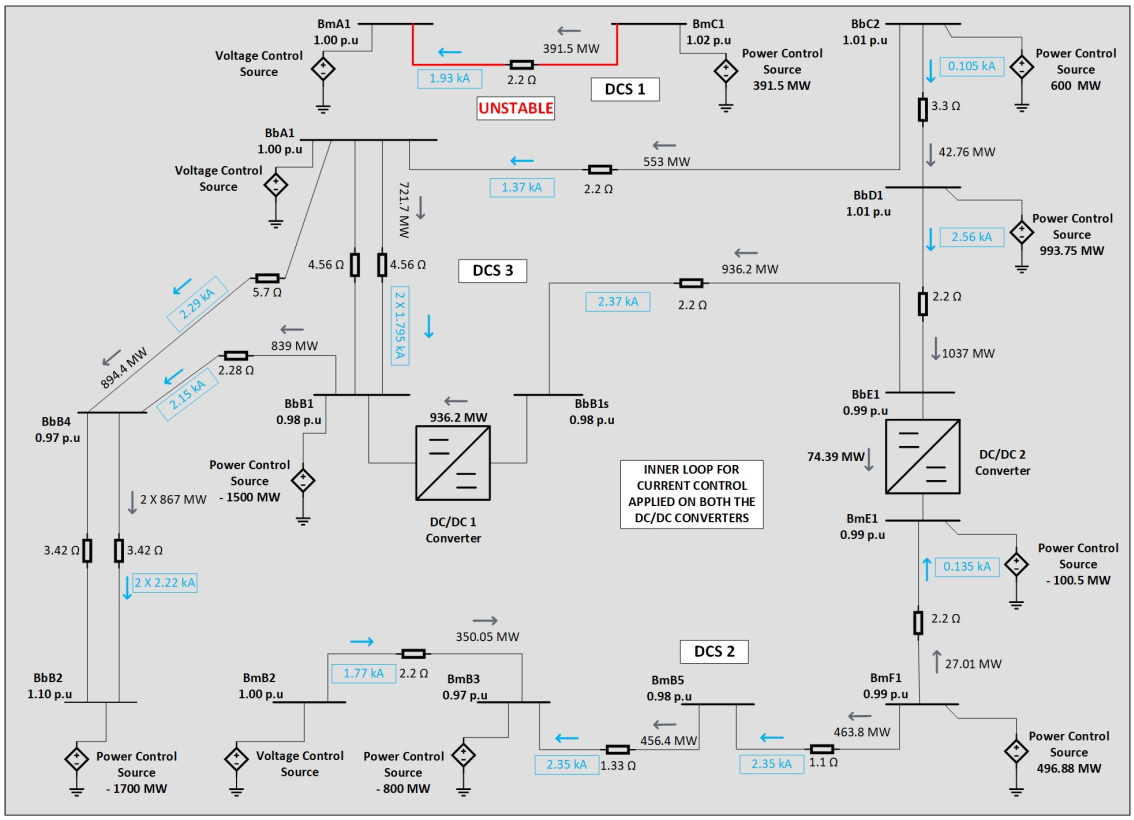

Figure 5.2: Critical DC Links in DCS 1 Subsystem

Table 5.3: DC Links in DCS 2 Subsystem.

Sr No.	DC Link		Type	Voltage (kV)
	From	To		
1	BmE1	BmF1	Sym. MP Cable	200
2	BmF1	BmB5	Sym. MP Cable	200
3	BmB5	BmB3	Sym. MP OHL	200
4	BmB3	BmB2	Sym. MP Cable	200

5.6 Contingency Analysis over DCS 2 Subsystem

The DCS 2 subsystem of the CIGRE DC Test Grid Model is a 4-terminal symmetric monopole HVDC system with voltage rating of +/- 200 kV. This system connects the offshore wind power plant (F1 terminal) and the offshore Oil & Gas platform (at E1 terminal) to the onshore node B3 and to load centre B2, as shown in Fig. 3.1 of Chapter 3. The four DC links are listed in Table 5.3.
In this system, a disconnection on all the four DC links is conducted with only an inner loop for current control applied on both the DC/DC converters.

The DCS 2 subsystem has a radial topology as shown in Section 2.5 of Chapter 2. As shown in Figure 5.1, the converters at DC buses BmE1 and BmB3 are in power control mode and draw 100.5 MW and 800 MW, respectively. The converter

at DC bus BmF1 is in power control mode and injects 496.88 MW into the DC grid. The converter at DC bus BmB2 is in voltage control mode.

In considering contingencies in this subsystem, a disconnection of any of the cascaded network of DC links causes an increase in current over the adjacent DC links leading to increase in DC bus voltages beyond the permissible limits (> 1.05 p.u). This happens as the converters at the DC buses are injecting or drawing power at their rated capacities. Due to this, current overloading of the DC links is observed as well. To maintain the DC voltage in the permissible range between any of the cascaded DC links following a disconnection, there is no DC bus which can hold the voltage constant. The absence of a voltage control causes the grid becomes unstable. Correspondingly, as both the DC/DC converters are using inner loops for current control, the PI controllers are not able to rectify the large error in the reference and actual current leading to their saturation.

Since the disconnection of these DC links lead the grid to become unstable, these DC links are classified to be *Critical* DC links. Figure 5.3 shows the *Critical* DC links with inner loop for current control applied on both the DC/DC converters.

Thus, to mitigate this instability, the DC/DC converters are implemented outer loop control for voltage (using voltage control and/or voltage step ratio control).

The DC/DC 2 converter is now applied with an an outer loop for voltage control, as explained in Section 4.5 of Chapter 4, with a set-point of 1 p.u (200kV) as shown in Figure 5.5. In other words, the reference signal to the the outer loop is set as 200 kV. Following a contingency on any of the DC link, the increase in DC link current causes corresponding DC bus voltage to increase as well. This increase of voltage leads to a deviation for the voltage controller reference, which acts by discharging the DC/DC converter's capacitor until the measured voltage equals equals the set point. In that way, the DC bus voltage is controlled. Hence, the presence of voltage control mitigates the grid instability and regulates the DC power flow. However, it should be observed that although the DC bus voltages are now regulated, the DC links will be overloaded.

A case study of a disconnection of DC link BmE1 to BmF1 is presented.

5.6.1 Case Study - Disconnection of DC Link BmE1 to BmF1

The DC link from BmE1 to BmF1 is connected between converters at DC buses BmE1 (drawing 100.5 MW) and BmF2 (injecting 496.88 MW). In steady state operation, the DC link carries 27.01 MW from BmF1 to BmE1.

With both the DC/DC converters applied with inner loop for current control, following a disconnection of this DC link, as shown in Figure 5.4, the voltage at DC bus BmE1 dips below the permissible limit. Further, the cascaded DC links from

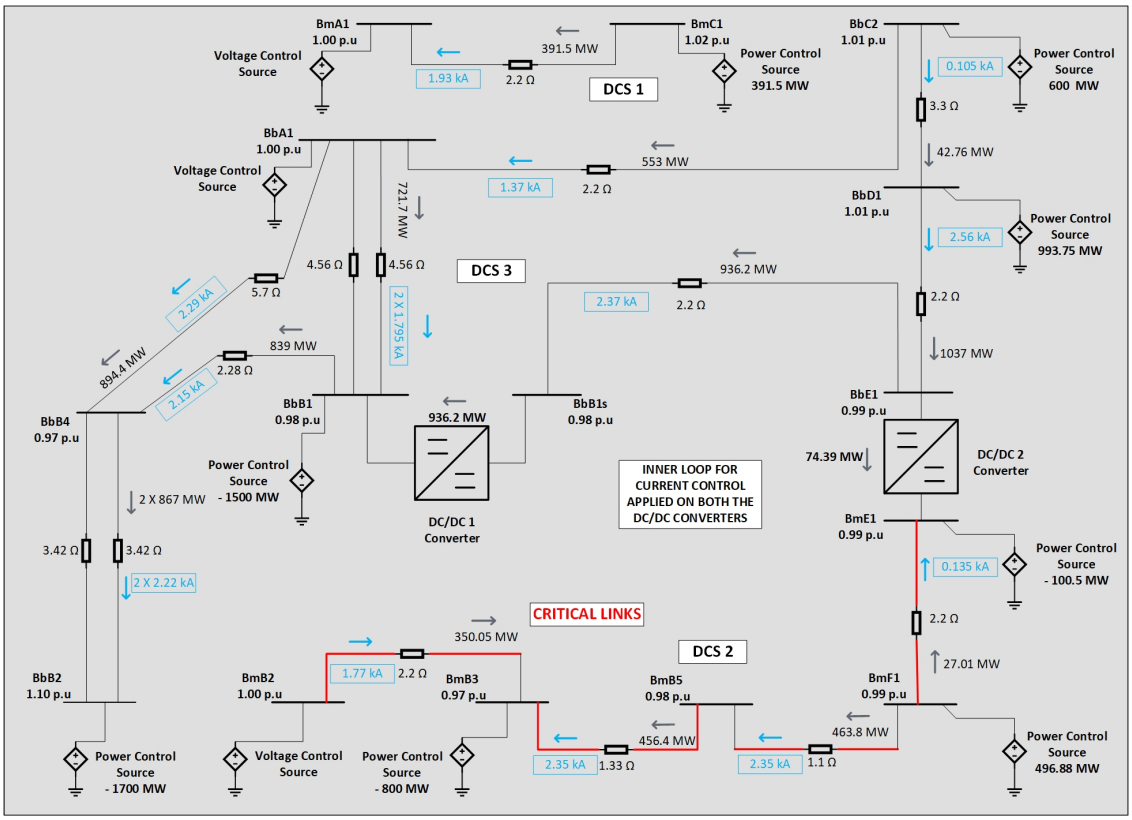

Figure 5.3: Critical DC Links in DCS 2 System

BmF1 to BmB3 experience a surge in current leading to their overloading. Correspondingly, due to no voltage control present at BmE1, the subsystem becomes unstable, leading to the entire DC grid becoming unstable.

With the outer loop for voltage control now applied at both the DC/DC converters, the voltage at the DC Bus BmE1 is successfully maintained at a set point of 1 p.u (200kV), as shown in Figure 5.5. The DC power flow is now regulated between the cascaded network of DC buses BmF1 to BmB2, as the converter at DC bus BmB2 is in voltage control mode. However, although the DC buses are voltage regulated, the disconnection of DC link still causes the adjacent DC links to become overloaded.

Correspondingly, a contingency on any of the other radial DC links (BmF1 to BmB5, BmB5 to BmB3 and BmB3 to BmB2) does not turn the grid unstable as there is always a converter that is in voltage control mode. Hence, by applying the DC/DC converters with outer loop for voltage control promotes the *Critical* DC links to becoming *Non Critical* DC links in the DCS 2 subsystem.

It should be observed here that although the applied voltage control does maintain the DC buses to be within permissible limits, the DC links are still subjected to overloading following a disconnection, and should be disconnected from the grid, or power injections from the converters should be reduced.

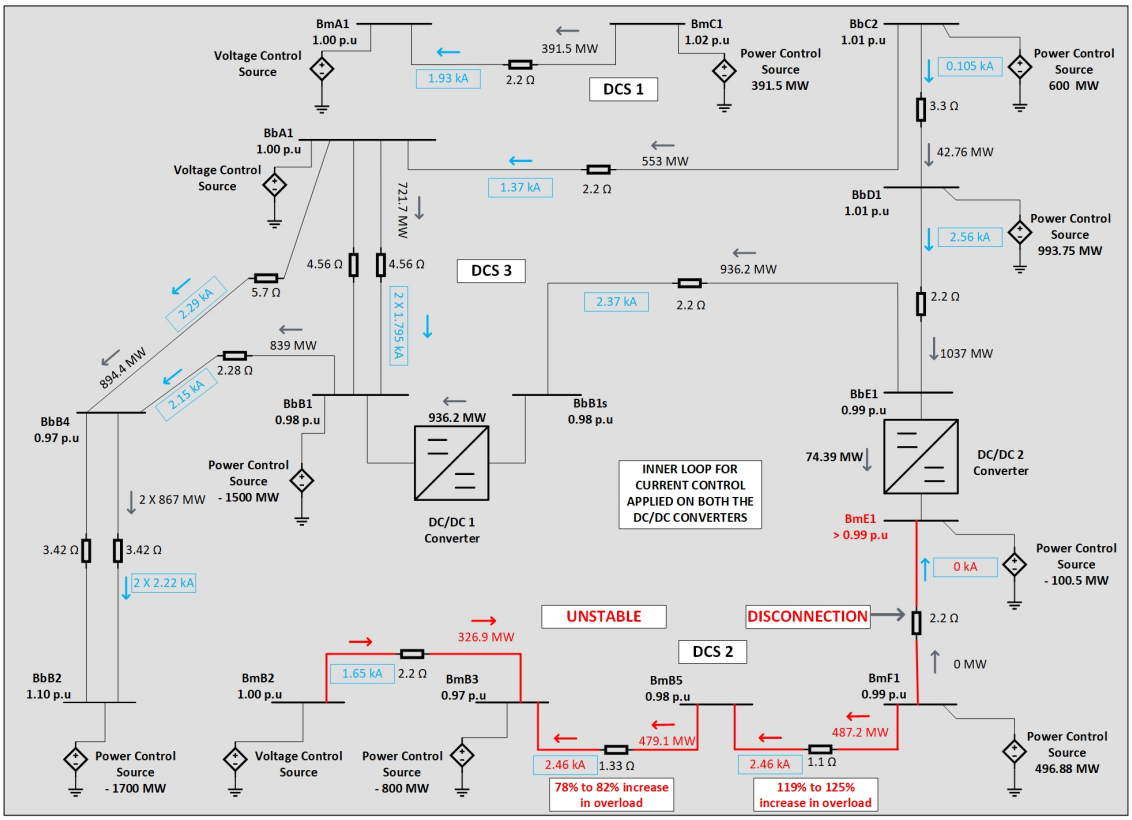

Figure 5.4: Contingency on DCS 2 Case Study

Similar results are obtained when outer loop using voltage step ratio control is applied on both DC/DC converters, wherein the DC bus voltage is regulated within permissible value. In using a voltage step ratio as the outer loop, oscillations are observed before a steady state is reached following a contingency.

Section A.6 of Appendix A shows the graphs of output power with oscillations in PSCAD.

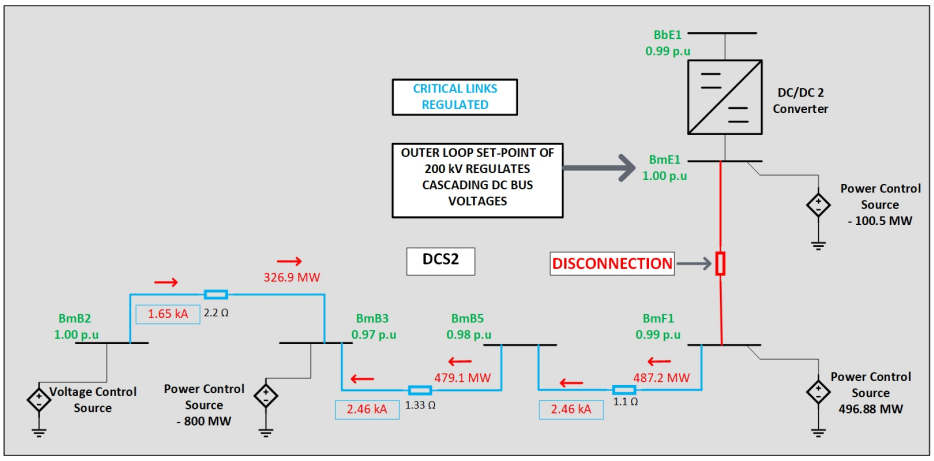

Figure 5.5: Outer Loop applied on DCS2

It important to notice here that in case of a contingency on the DCS 2 subsystem, the outer loop for voltage control applied on DC/DC 1 converter plays a minimal role. This is due to the fact that once the voltage over the bus BmE1 is regulated to 1.00 p.u, the voltage over BbE1 will be regularised to *2.00 p.u* owing to power-balance, since the DCS 3 system is rated at +/- 400kV, while the DCS 2 system is rated at +/- 200kV. The voltage over the DC link connecting the two DC/DC converters is maintained between acceptable values.

5.7 Contingency Analysis over DCS 3 Subsystem

The DCS 3 subsystem of the CIGRE DC Test Grid Model is a 5-terminal bipole meshed HVDC system with voltage rating of +/- 400 kV with a total of 8 DC links. The converters at DC buses BbB1 and BbB2 are in power control mode and draw 1500 MW and 1700 MW, respectively, from the DC grid. The converters at DC buses BbC2 and BbD1 are in power control mode as well and inject 600 MW and 993.75 MW, respectively, into the DC grid. These power injections are from the wind farms connected at the terminals of these converters. The converter at DC bus BbA1 is in voltage control mode. The eight DC links are listed in Table 5.4.

In this system, a disconnection on all the eight DC links is conducted with only an inner loop for current control applied on both the DC/DC converters. The two parallel OHL DC links are considered as a single unit.

Similar to the DCS 2 subsystem, in considering contingencies on the DCS 3 subsystem, a disconnection of any of DC links that are directly connected to a power controlled source cause an increase in current over the adjacent DC links leading to increase in DC bus voltages beyond the permissible limits ($>$ 1.05 p.u). This happens as the converters at the DC buses are either injecting or drawing power at their rated capacities. To maintain DC voltage between any of these DC links following a disconnection, there is no converter at a DC bus that is in voltage con-

Table 5.4: DC Links over DCS 3 system.

Sr No.	DC Link		Type	Voltage (kV)
	From	To		
1	BbA1	BbC2	Bipole Cable	400
2	BbC2	BbD1	Bipole Cable	400
3	BbD1	BbE1	Bipole Cable	400
4	BbE1	BbB1s	Bipole Cable	400
5	BbB1	BbB4	Bipole OHL	400
6	BbA1	BbB1	Bipole OHL X 2	400
7	BbA1	BbB4	Bipole OHL	400
8	BbB2	BbB4	Bipole OHL x 2	400

trol mode. which can hold the voltage constant. The absence of a voltage control causes the grid to become unstable. Correspondingly, as both the DC/DC converters are using inner loops for current control, the PI controllers are not able to rectify the large error in the reference and actual current further leading to their saturation.

Since the disconnection of these DC links lead the grid to become unstable, these DC links are classified to be *Critical* DC links and are subjected to outer loop control for voltage or voltage step ratio.

In considering contingencies on the DCS 3 subsystem, a disconnection of any of DC links that are directly (or via a DC bus) connected to a voltage controlled source do not cause an increase in current over the adjacent DC links. The DC bus voltages over the rest of the subsystems remain within permissible limits (0.95 - 1.05 p.u). This happens as there is always a converter at a DC bus which is voltage control mode, following the disconnection. The presence of voltage control causes the grid to remain stable and thus regulate the power flow over the healthy part of the DC grid. Correspondingly, as both the DC/DC converters are using inner loops for current control, the PI controllers are able to rectify the error in the reference and actual current and mitigating instability in the DC grid.

Since the disconnection of these DC links does not lead the grid to become unstable, these DC Links are classified to be *Non Critical* DC links and are not subjected to outer loop control for voltage or voltage step ratio.

Figure 5.6 shows the *Critical* and *Non Critical* DC links with inner loops for current control applied on both the DC/DC converters.

The DC/DC 1 converter is now applied with an an outer loop for voltage control, as explained in Section 4.5 of Chapter 4, with a set-point of 1 p.u (393.83kV). In other words, the reference signal to the the outer loop is set as 393.83kV as shown in Figure 5.8. Following a contingency on any of the *Critical* DC link, the increase

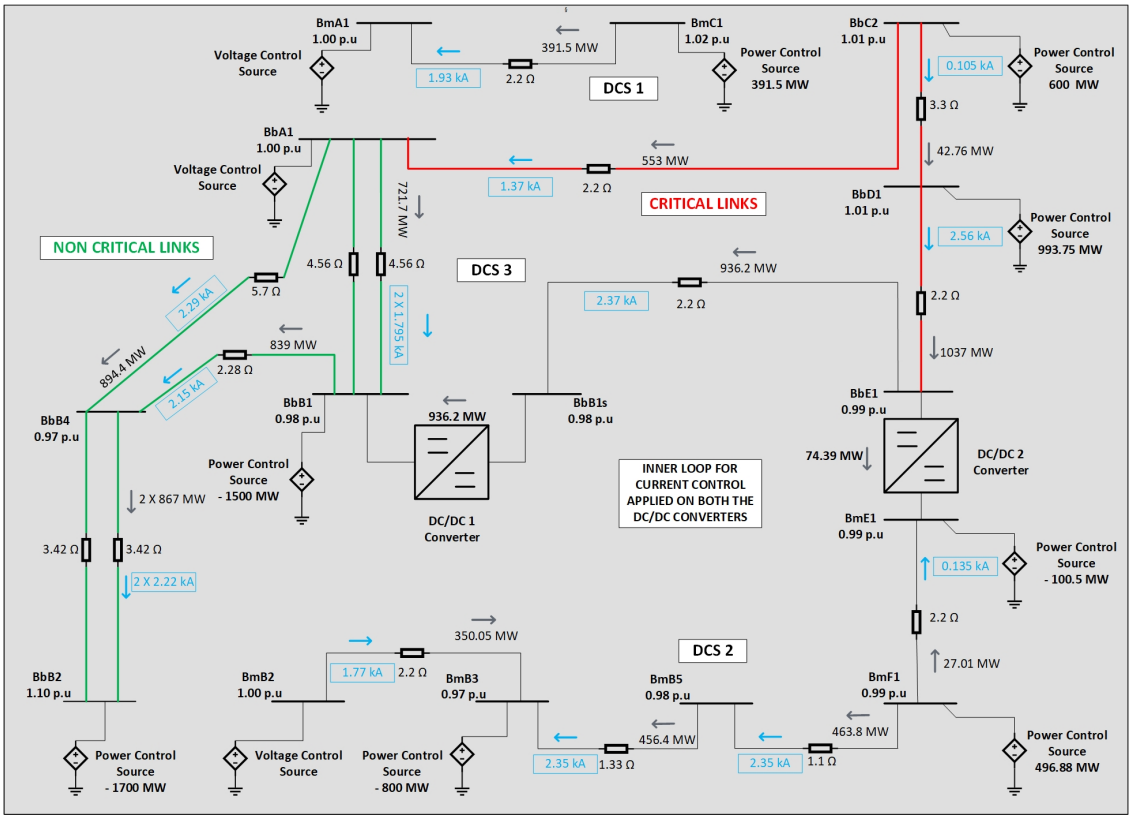

Figure 5.6: Critical and Non Critical DC Links in DCS 3 Subsystem

in DC link current causes corresponding DC bus voltage to increase as well. This increase of voltage leads to a deviation for the voltage controller reference, which acts by discharging the DC/DC converter's capacitor until the measured voltage equals equals the set point. In that way, the DC bus voltage is controlled. Hence, the presence of voltage control mitigates the grid instability and regulates the DC power flow. However, it should be observed that although the DC bus voltages are now regulated, the DC links will be overloaded.

To explain the same in detail, a case study of a disconnection of DC Link BbC2 to BbA1 is presented below.

5.7.1 Case Study - Disconnection of DC Link BbC2 to BbA1

The DC link from BbC2 to BbA1 is connected between converters at DC buses BbC2 (injecting 600 MW) and BbA1 (voltge control mode). In steady state operation, the DC link carries 553 MW from BbC2 to BbA1.

With both the DC/DC converters applied with inner loop for current control, a disconnection of this DC link, as shown in Figure 5.7, the voltage at DC bus BbC2 rises above the permissible limit. Further, the cascaded DC links from BbC2 to BbE1 and further to DC/DC 2 converter experience a surge in current leading to their overloading. Correspondingly, due to no voltage control present at BbE1, the

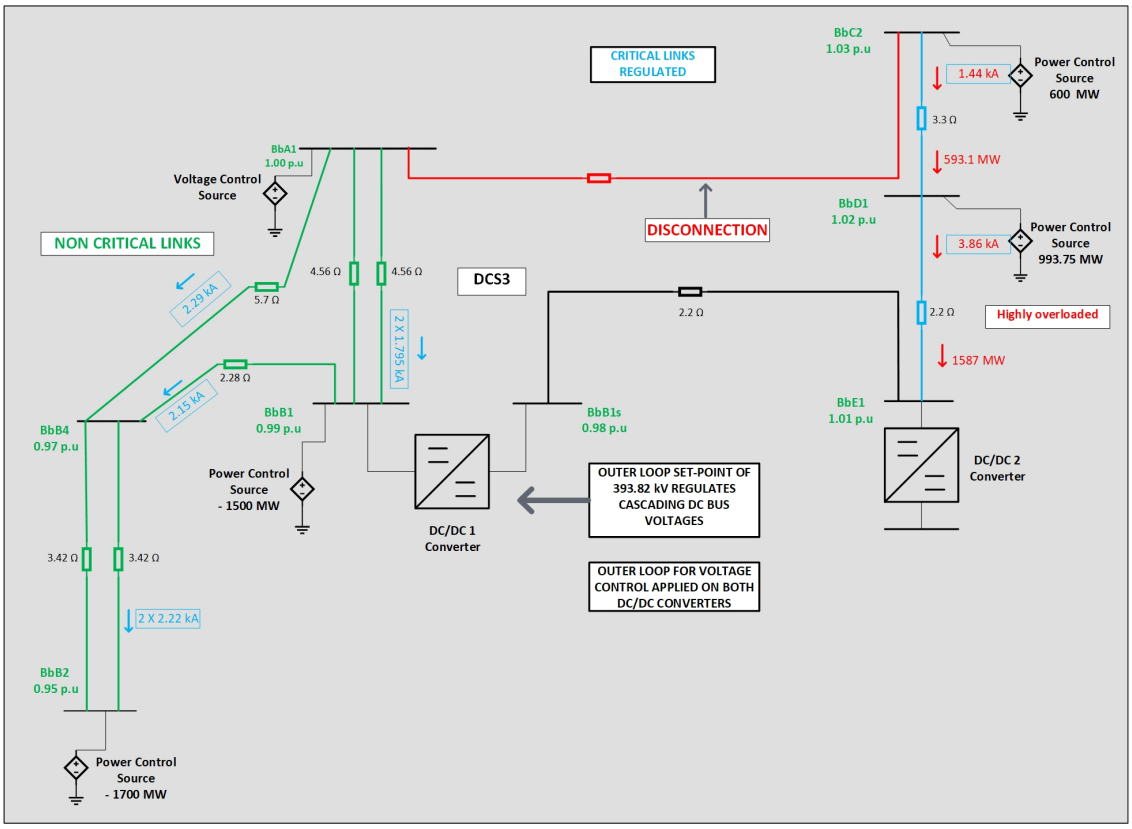

Figure 5.7: Outer Loop applied on DCS 3

subsystem becomes unstable, leading to the entire DC grid becoming unstable. Since there is no voltage control present at the DC/DC converter, the DCS 2 subsystem is also affected by the surge in power.

With the outer loop for voltage control now applied at both the DC/DC converters, the voltage at the DC Bus BbB1s is successfully maintained at a set point of 1 p.u (393.92kV), as shown in Figure 5.8. Further, the voltage at the DC Bus BbB1 is also successfully maintained at a set point of 1 p.u (200kV). The DC power flow is now regulated between the meshed network, as the converter at DC bus BbA1 is in voltage control mode. However, although the DC buses are voltage regulated, the disconnection of DC link still causes the adjacent DC links to become overloaded.

Correspondingly, a contingency on any of the other the other DC links (BbC2 to BbD1, BbD1 to BbE1) does not turn the grid unstable as there is always a converter at a DC bus that is in voltage control mode. Hence, by applying the DC/DC converters with outer loop for voltage control promotes the *Critical* DC links to becoming *Non Critical* DC links in the DCS 3 subsystem.

It should be observed here that although the applied voltage control does maintain the DC buses to be within permissible limits, the DC links are still subjected to overloading following a disconnection, and should be disconnected from the grid, or power injections from the converters should be reduced.

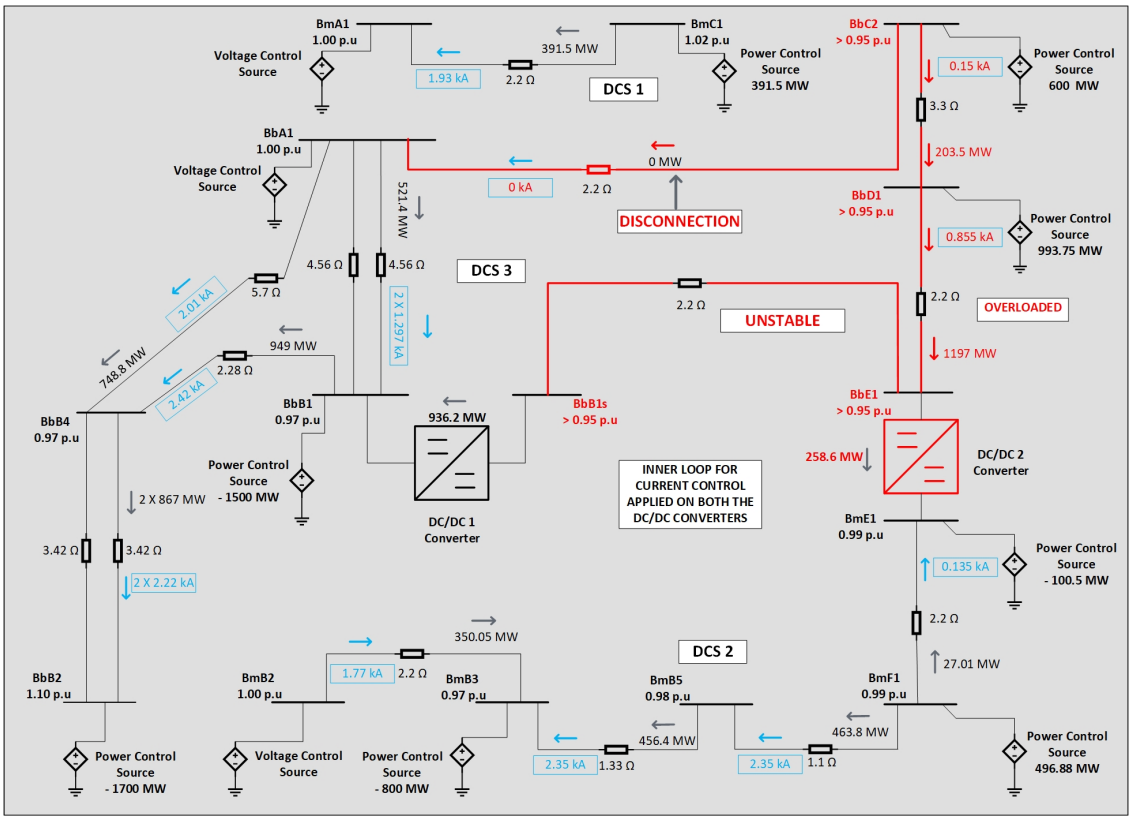

Figure 5.8: Contingency on DCS 3 Case Study

Similar results are obtained when outer loop using voltage step ratio control is applied on both DC/DC converters, wherein the DC bus voltage is regulated within permissible value.

It important to notice here that in case of a contingency on the DCS 3 subsystem, the outer loop for voltage control applied on DC/DC 2 converter plays a minimal role. This is due to the fact that once the voltage over the bus BbB1s is regulated to 1.00 p.u, the voltage over DC bus BmE1, through DC bus BbE1 will be regularised to *0.5 p.u*, since the DCS 2 system is rated at +/- 200kV, while the DCS 3 system is rated at +/- 400kV. The voltage over the DC link connecting the two DC/DC converters is maintained between acceptable values.

6

Further on Steady State Contingency Analysis

This chapter describes further considerations for the contingency analysis conducted on the CIGRE DC Grid Test Model.

6.1 Introduction

In the previous chapter, contingency analysis over each of the 13 DC links on the CIGRE DC Grid Test model has been conducted. It has been found that when only an inner loop for current control is applied over both the DC/DC converters, grid instability occurs following a disconnection in any of the *Critical* DC links. This occurs mainly since there is no voltage control present to regulate the DC power flow. However, the grid remains stable when any of the *Non Critical* DC links are disconnected as some of the converters are in voltage control mode. The grid instability can be mitigated by applying an outer loop for voltage control (either with Voltage Control or Voltage Step Ratio Control).

In this chapter, observations about applying selective control strategies on the DC/DC converters are presented. Further, special cases of using a Modified Step Control using *Selective Loop Technique* in case of non-stiffness of DC voltages from the VSCs, cases of *varying power inputs*, cases of *power set-points* for the DC/DC converters and DC power flow with *additional DC Links* in DCS 2 & DCS 3 subsystems are studied as well.

6.2 Selective Control Strategies

It is observed that a contingency on a particular DCS subsystem mainly affects the DC power flow in that subsystem, while the rest of the subsystems in the DC grid remain relatively unaffected.

Consider the DCS 2 subsystem with both DC/DC converters implemented only with inner loop for current control. When a disconnection was created on any of the *Critical* DC links as shown in in Figure 5.3, the grid instability was caused as there was no voltage control to regulate the DC buses. Since the error signal was too large to rectify, the PI controllers in control loops on the DC/DC 2 converter progressed towards saturation, which eventually led to the PI controllers in control

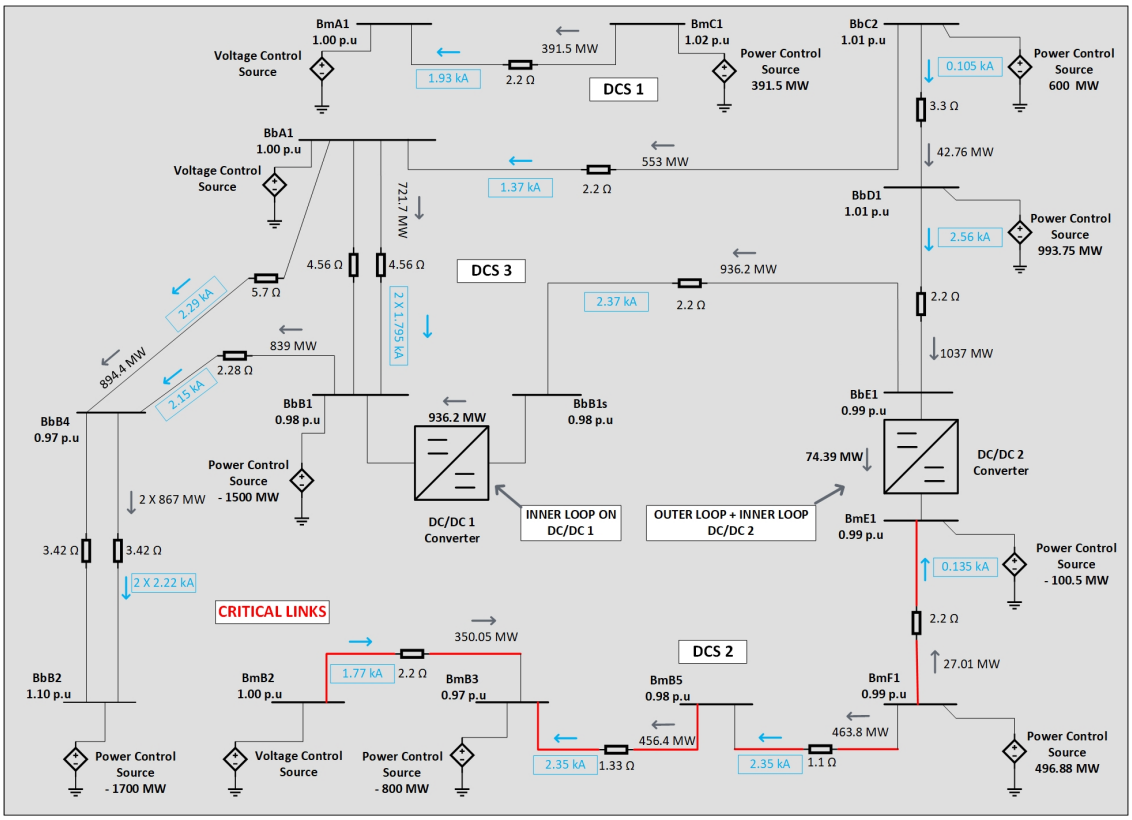

Figure 6.1: Selective Control on DCS2 Subsystem

loops on the DC/DC 1 converter to progress towards saturation as well.

When an outer loop for voltage control was applied over the DC/DC 2 converter to rectify a *Critical* contingency made in the DCS 2 subsystem, the voltage control was effective in maintaining DC bus voltages in the DCS 2 subsystem. Correspondingly, the capacitors were able to discharge till the measured voltage was equal to the set-point and the subsystem was balanced. The cascaded PI controllers were able to rectify the error signal as well. Since the voltage over the DC link between the DC/DC converters (BbE1 to BbB1s) was being maintained by DC/DC 2, inner loop for current control over DC/DC 1 was found to be sufficient in maintaining stability over the DCS 3 subsystem.

Hence it was analysed that contingencies over the DCS 2 subsystem would only require outer loop for voltage control on DC/DC 2 converter for instability mitigation, while inner loop for current control on the DC/DC 1 converter can still be sufficient for maintaining stability over DCS 3 subsystem. The simulation results in Figure 6.1 show that mitigation of instability in DCS 2 subsystem will only require outer loop for voltage control DC/DC 2 converter only.

Similarly, consider the DCS 3 subsystem with both DC/DC converters implemented only with inner loop for current control. When a disconnection was created on any

of the *Critical* DC links as shown in in Figure 5.6, the grid instability was caused as there was no voltage control to regulate the DC buses. Since the error signal was too large to rectify, the PI controllers in control loops on the DC/DC 1 converter progressed towards saturation, which eventually led to the PI controllers in control loops on the DC/DC 2 converter to progress towards saturation as well.

When an outer loop for voltage control is applied over the DC/DC 1 converter to rectify a *Critical* contingency made in the DCS 3 subsystem, the voltage control was effective in maintaining DC bus voltages in the DCS 3 subsystem. Correspondingly, the capacitors were able to discharge till the measured voltage was equal to the set-point and the system was balanced. The cascaded PI controllers were able to rectify the error signal as well. Since the voltage over the DC link between the DC/DC converters (BbE1 to BbB1s) was being maintained by DC/DC 1 converter, inner loop for current control over DC/DC 2 was sufficient in maintaining stability over the DCS 2 subsystem.

Hence it was analysed that for contingencies over DCS 3 subsystem would only require outer loop for voltage control over DC/DC 1 converter for rectification, while inner loop over DC/DC 2 converter can still be sufficient for maintaining stability over DCS 2 subsystem. The simulation results in Figure 6.2 show that mitigation of instability in DCS 3 subsystem will only require outer loop for voltage control DC/DC 1 converter only.

Using voltage step ratio for outer loop showed similar results for both, DCS 2 and DCS 3 subsystems, although the DC bus voltages oscillated before reaching a steady-state. It should be noted here that the model developed is meaningful only for steady state analysis. A special case of using voltage step ratio is explained in the next section.

6.2.1 Special Case of Contingency over BbD1 to BbE1 DC Link

As explained in the previous section, following in contingency in one DCS subsystem, only an outer loop applied using voltage step ratio control on DC/DC converter for that system would rectify DC bus voltages and mitigate instability. However, in this special case the instability in the grid caused by a contingency applied over the *Critical* DC link in the DCS 3 subsystem (BbD1 to BbE2) can be rectified by applying outer loop over DC/DC 2 instead of DC/DC 1 to mitigate instability. The DC/DC 1 converter can be only applied with inner loop for current control to maintain grid stability.

In this case, since outer loop for voltage step control is applied over DC/DC 2, the voltage at the DC bus BbE1 will be rectified to its set-point value of 393.82 kV (0.98 p.u). Due to the controlling action of the outer loop, the current over the DC link connecting both the DC/DC converters is maintained and the voltage on DC bus BbB1s is regulated. Hence, the DC/DC 1 converter is able to maintain stability

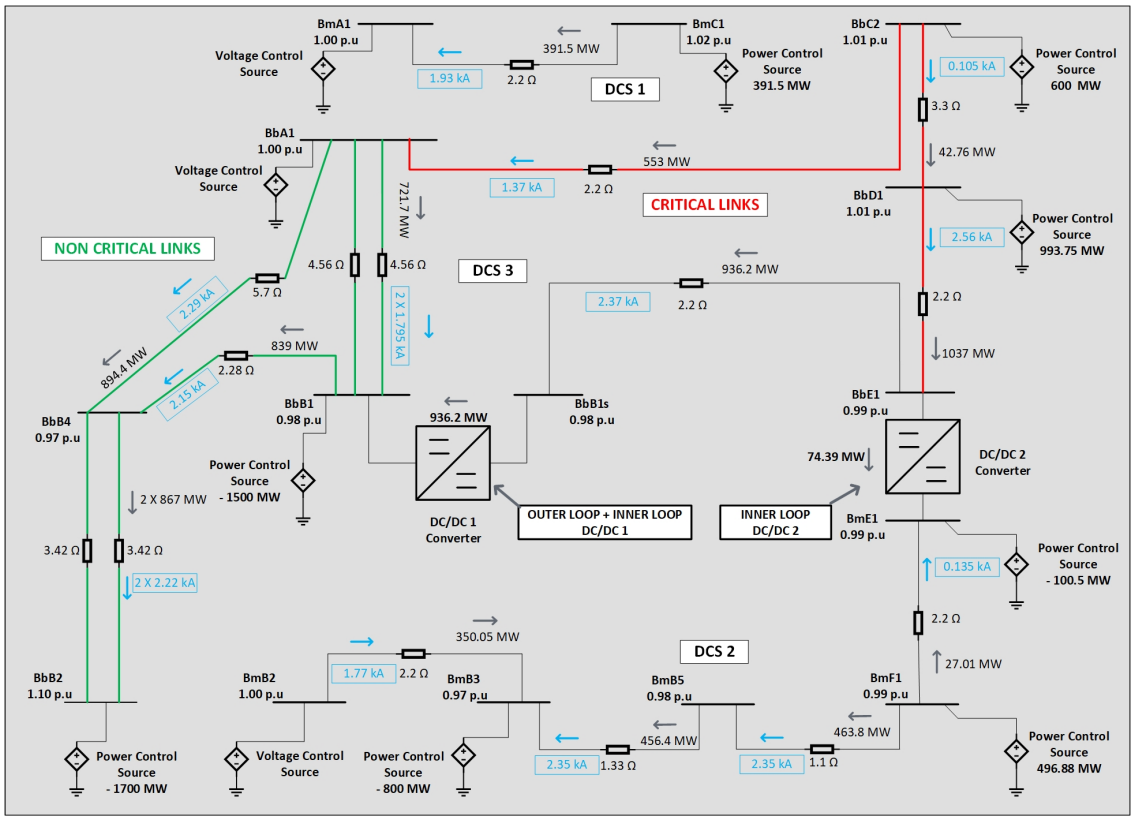

Figure 6.2: Selective Control on DCS 3 Subsystem

over the DCS 3 system only with inner loop for current control applied, as shown in Fig. 6.3.

Using voltage step ratio as the outer loop can help in cases where a new DC link needs to be integrated into the MTDC grid. In this case, the DC/DC converter will act as a voltage controlled source at receiving end for the DC link to be integrated. However, when this outer loop is applied to a DC/DC converter that is connected to a VSC which is in voltage controlled mode, DC stability could be affected by the stiffness of the DC voltage at the VSC.

6.3 Modified Step Control

The principle of voltage step ratio control in DC/DC converters is analogous to a certain voltage/winding ratio in an AC transformer, as explained in Section 4.5.2 of Chapter 4. By using a reference input of unity, this control loop rectifies the ratio of voltages at both ends of the DC bus connected to the DC/DC converter to be equal. Further, this principle can also be applied to step up or step down voltage across a DC/DC converter by setting appropriate reference set-points.

However, this method of control can adversely affect the stability of the DC grid in cases the VSCs that are directly connected to the DC/DC converter do not maintain

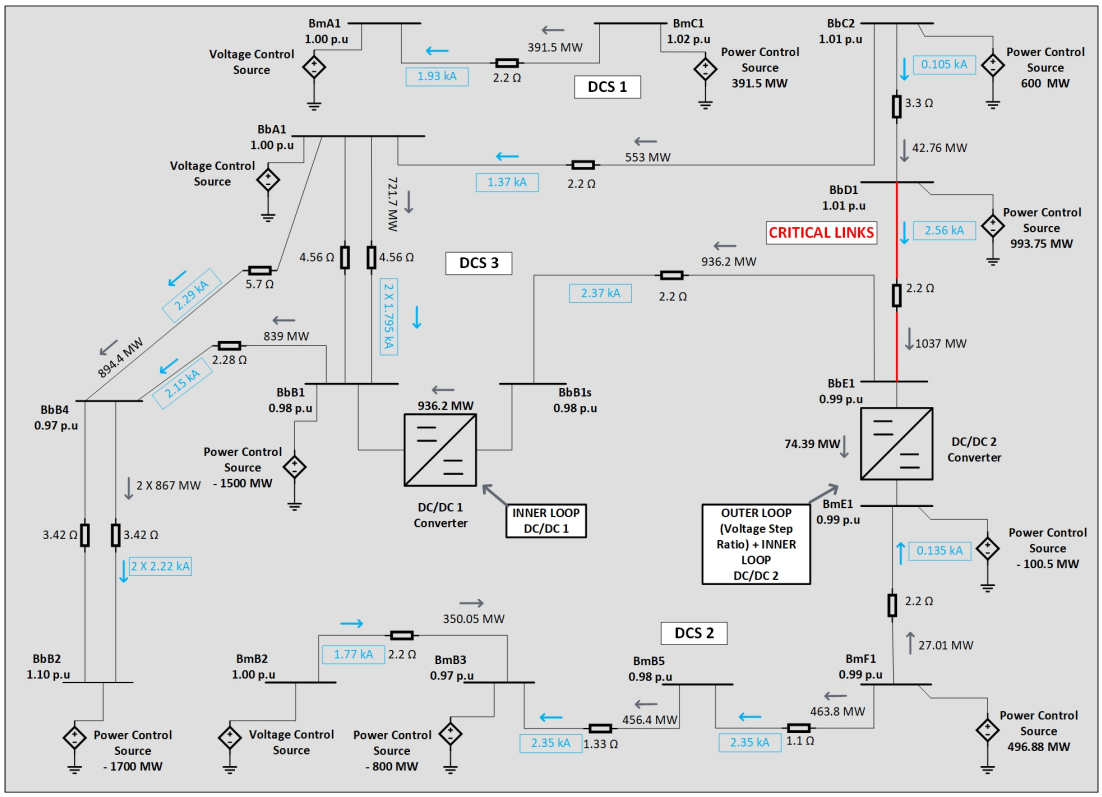

Figure 6.3: Special Case using Voltage Step Ratio Control over DC/DC 2 for a contingency in DCS 3 system

stiff DC values.

Consider the following scenarios:

- The DC/DC converter at one side is directly or via a bus link connected to a DC bus that is in voltage control mode. Further, for some reasons, the voltage at the VSC terminal dips, which makes the input voltage to this DC bus also dip below the acceptable range of 0.95 p.u. In this case, due to the outer loop applied using voltage step control on the DC/DC converter, the voltage dip will be further propagated to the to the DC bus on the other side of the DC/DC converter. This is due to the fact that the outer loop will simply maintain the voltage ratio to the set-point, without considerations for the permissible levels of DC voltage. This can cause a cascading effect of voltage drop in the DC bus network and further lead to overloading of the DC Link, or in worse case lead to a power reversal.

- Now considering the same case where the input voltage at the DC bus rises above the acceptable range of 1.05 p.u. In this case, due to the outer loop applied using step voltage control on the DC/DC converter, the voltage rise will be further propagated to the to the DC bus connected to the other side of the DC/DC converter. This can cause a cascading effect of voltage rise in the DC bus network and further lead to grid instability.

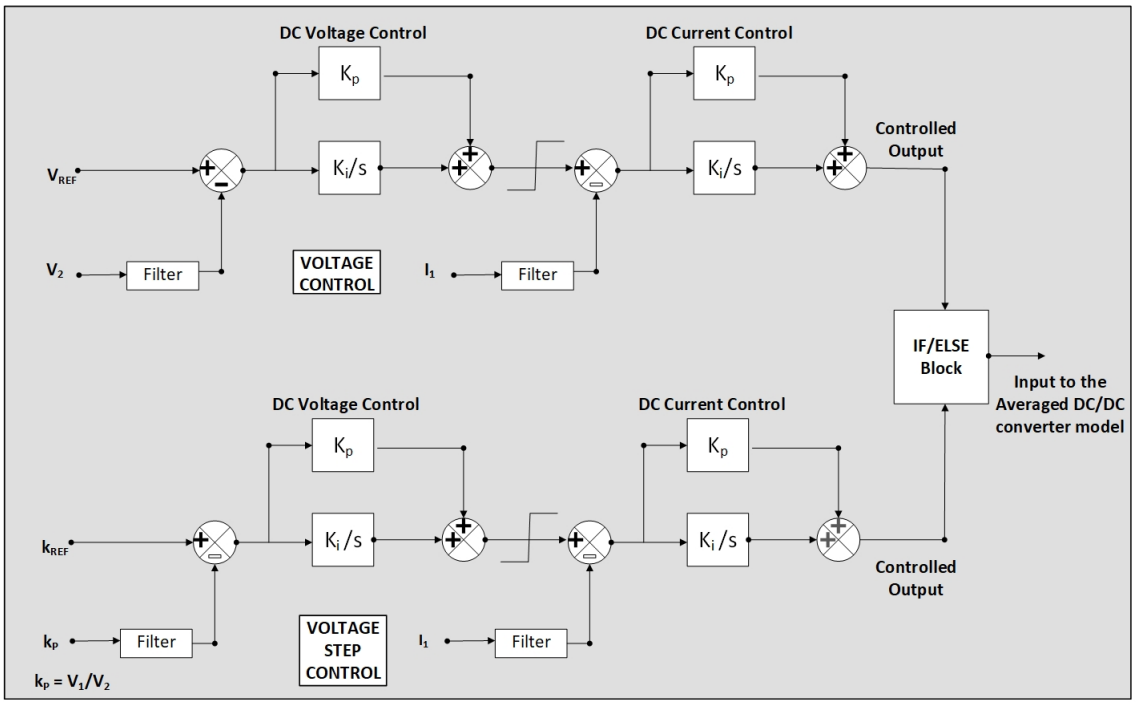

Figure 6.4: Selective Loop Technique using an IF-ELSE Function

To remove this inconsistency in applying voltage step control as the outer loop, a *Selective Loop Technique* is applied. This is explained in Figure 6.4, wherein two control loops are connected to an IF/Else selection block. Both of these are outer control loop, with voltage control and step-voltage control.

The IF/Else selection function is designed in such a way that the initial control loop will be voltage step control, when the voltage at both the DC buses is between the the permissible range. When the controller detects that the voltage at either of the DC bus on the DC/DC converter is not within the permissible range, it will swap the control loop to being voltage control mode. The voltage control mode will have a set-point that is 1 p.u, which will regulate the connected DC buses to 1 p.u. In this way, the cascading effect of the step-voltage control can be avoided. When the controller detects that the voltage is again within the permissible range, it can swap back the outer loop to voltage step control.

The *Selective Loop Technique* could be effectively applied in case the DC buses in voltage control mode often experience voltage variations.

6.4 Variations in Power Inputs

In this section, the developed DC grid of the CIGRE DC Grid Test Model is subjected to varying power inputs to inspect the stability of the DC grid in case the

Table 6.1: Varied input power over the DC busses.

Sr No.	Bus	System	Rated MW	Varied MW
1	BmF1	DCS 2	496.88	248.44
2	BmF1	DCS 2	496.88	993.76
3	BbC2	DCS 1	600	300
4	BbC2	DCS 1	600	600
5	BbD1	DCS 1	993.75	496.88
6	BbD1	DCS 1	993.75	1987.5

Wind Power Plants at the converter terminals are varying in output. Further, following a contingency over a *Critical* DC link, simulations are run to check if increasing or decreasing the input power on the converters at the DC buses can mitigate instability. Further, this is done with both the DC/DC converters applied only with inner loop for current control and not with outer loops for voltage control instead.

In other words, it is checked if instability caused by the disconnection of a *Critical* DC link in any of the DCS subsystems could be mitigated by directly varying the input power in that DCS subsystem through the converters at the DC buses, instead of using outer loop for voltage control on the DC/DC converters. Further, it is checked if doing so can assist in promoting a *Critical* DC link to becoming *Non Critical* DC link.

In the CIGRE DC Grid Test Model, there are three converter terminals connected to Wind Power Plants at bus BbC2, BdB1 and BmF1 injecting 600 MW, 993.75 MW and 496.88 MW, respectively, as can be seen from Figure 3.1 in Chapter 3 and Figure 5.1 in Chapter 5. With variations in power input to the DC grid at these three busses, test cases are motivated as shown in Table 6.1. The power is varied to half and twice its rated value following a contingency over a *Critical* DC link in that particular DCS system.

It was found that varying the power input did not succeed in in promoting a *Critical* DC link to becoming *Non Critical* DC link.

In order to exchange power over a point-to-point HVDC link, it is necessary to have a VSC in voltage control mode at one end and the other VSC in power control mode at the other end [7]. As observed in the previous chapter, in the disconnection of *Critical* DC links over both the DCS subsystems, the DC grid becomes unstable when there is no voltage control present to regulate the DC power flow. When the input power was varied over the DC grid following disconnection of a *Critical* DC link, it resulted in decreasing the current flow but the lack of voltage control resulted in DC grid instability.

Since the variance of power input cannot promote a *Critical* DC link to being *Non Critical*, further investigation regarding varying power over the DC/DC converters is conducted.

Table 6.2: Step Responses in DC/DC converters

Sr No.	Converter	System	Rated MW	Transfer MW	Varied MW
1	DC/DC 1	DCS 3	2000	936.2	1500
2	DC/DC 1	DCS 3	2000	936.2	500
3	DC/DC 2	DCS 2	1000	73.83	500
4	DC/DC 2	DCS 2	1000	73.83	750

6.5 Step Responses in DC/DC converters

In the steady state contingency analysis for DC power flow conducted in Chapter 5, the DC/DC converters were given current set-points based the uncontrolled power flow, as described in Section 3.4 of Chapter 3. The values for the same were obtained as per Table 3.6 of Chapter 3.

In this section, the DC/DC converters are subjected to step responses to inspect the stability of the DC grid following disconnection of a *Critical* DC link. The current set-points over the DC/DC converters are changed to half and twice their values, as shown in Table 6.2. This is done in order to vary the power flow through the DC/DC converters. Both the DC/DC converters are applied with inner loop for current control.

As per the CIGRE DC Grid Test Model shown in Figure 3.3 in Chapter 3, the DC/DC 1 converter is rated at 2000 MW and the DC/DC 2 converter is rated at 1000 MW [27]. Considering steady state DC power flow analysis described in Section 5.1 of Chapter 5, the DC/DC 1 converter has a power transfer rating of 936.2 MW and DC/DC 2 converter has a power transfer rating of 73.82 MW.

Following disconnection of *Critical* DC link in both DCS 2 and DCS 3 subsystem, simulations are run to analyse if an increase or decrease in the power (using current set points) over the DC/DC converter can help mitigate DC grid instability. In other words, can varying power over the DC/DC converters following a *Critical* DC link disconnection promote that *Critical* DC Link to becoming *Non Critical* DC link.

In case of step responses over the DC/DC converter 1 in the DCS 3 subsystem, the disconnection of any of the *Critical* DC links made the DC grid unstable, due to lack of a converter in voltage control mode. The increase or decrease in power set-point did not promote any of the *Critical* DC link to becoming *Non Critical* as there was no voltage control present that could regulate DC power flow and mitigate instability in the DC grid.

Further, to compensate for the DC power loss, it was observed that increasing the power set-point over the DC/DC converter could further overload the adjacent DC links. In case of step responses over the DC/DC converter 2, similar results were obtained.

6.6 Variations in Power Inputs with Step Responses in DC/DC converters applied with Outer Loop

In sections 6.4 and 6.5, it was found that following a disconnection of Critical DC link, the lack of voltage control in in the DC grid let to its instability.

In this section of the report, the DC/DC converters are applied with outer loop for voltage control in order to regulate the DC power flow and mitigate the DC grid instability, following disconnection of a Critical DC link. Further, following that disconnection, simulations are run to analyse if step responses in DC/DC converters along with variations in power input can assist in decreasing overloading of adjacent the DC links, once the DC grid achieves steady state.

It was found that varying the power input along with step responses in the DC grid successfully decreased the loading of the adjacent DC link. Sample case studies of one of the *Critical* are presented.

6.6.1 Case Study - Disconnection of DC Link BmE1 to BmF1

The DC link from BmE1 to BmF1 is connected between converters at DC buses BmE1 (drawing 100.5 MW) and BmF2 (injecting 496.88 MW). In steady state operation, the DC link delivers 27.01 MW from BmF1 to BmE1 DC bus terminals. As can be seen in Figure 5.4 of Chapter 5, the disconnection of this DC link causes the adjacent DC links to be overloaded. Correspondingly, if the power injection at the converter at DC bus BmF1 is reduced to half its value (496.88 MW to 250 MW), the overloading of the adjacent DC links (BmF1 to BmB5, BmB5 to BmB3) can be significantly reduced, as shown in Figure 6.5. However, to satisfy the load at DC bus BmB3, the DC link from BmB2 to BmB3 becomes overloaded. This can be avoided if, along with reducing the power injection at DC bus BmF1, the power draw at DC bus BmB3 is reduced according to the rated capacity of the DC link. Further, in order to meet the load requirement at the converter at DC bus BmE1, the power output of the DC/DC 2 converter is increased from 73.82 MW to 102 MW to provide 27.01 MW of power, that was initially being delivered by the disconnected DC link.

6.7 Case Studies with Additional DC Links

As observed in Section 6.4 and Section 6.5, with both the DC/DC converters applied only with inner loop for current control, the variations in input power and step responses in DC/DC converter were found to be unsuccessful in mitigating DC grid instability, following disconnection of a *Critical* DC link. Considering that only by applying outer loops for voltage control on the DC/DC converters mitigate DC grid instability by providing voltage control, it is investigated if application of additional DC links that could maintain voltage control and re-distribute power flow could be applied for mitigating DC grid instability as well.

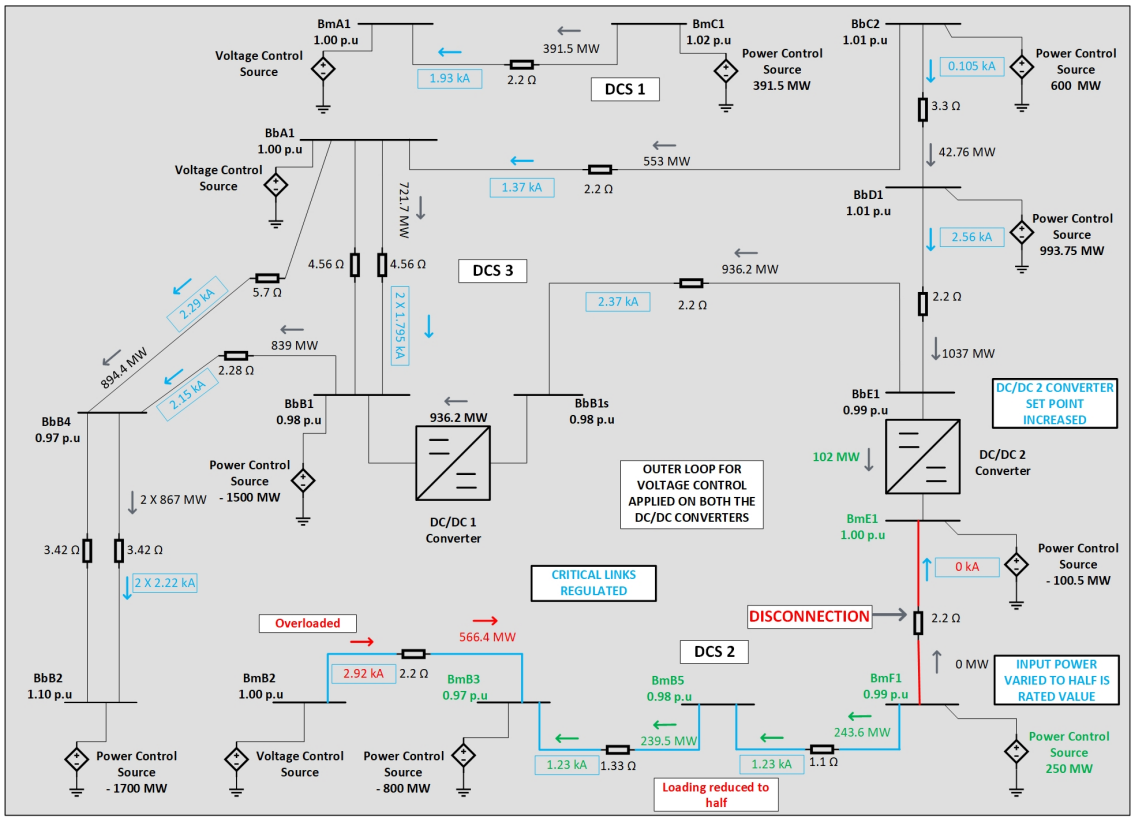

Figure 6.5: Varied Power Input on Critical DC link in DCS 2 Subsystem

The CIGRE DC Grid Test Model is developed to provide a common reference point for all the research over MTDC grids to have a coherent platform for development [27]. To further analyse the system and the robustness of the control strategies developed in this thesis, additional DC inks are strategically applied to the system. The principle followed is to create a bypass DC Link that could maintain voltage control and redistribute the DC power, thereby promoting a *Critical* DC link to becoming *Non Critical*.

As mentioned previously, DCS 1 system is *DC Decoupled* from DCS 2 and DCS 3 subsystems, hence is not considered in this analysis.

6.7.1 Additional DC Links in DCS 2 Subsystem

From the steady state contingency analysis conducted in Chapter 5, it was found that all the four DC links in this subsystem were *Critical*, as they formed a radial topology. The disconnection of any of them led to a loss of voltage control which made the DC grid unstable. To further test the system stability with only current control loops, an additional DC Link directly from the offshore wind power plant at E1 to load centre at B2 is implemented. The cable used is a DC symmetrical overhead monopole line. As shown in Figure 6.6, adding a DC Link from BmE1 to BmB3 makes the DCS 2 system a meshed DC grid topolgy from a radial topology.

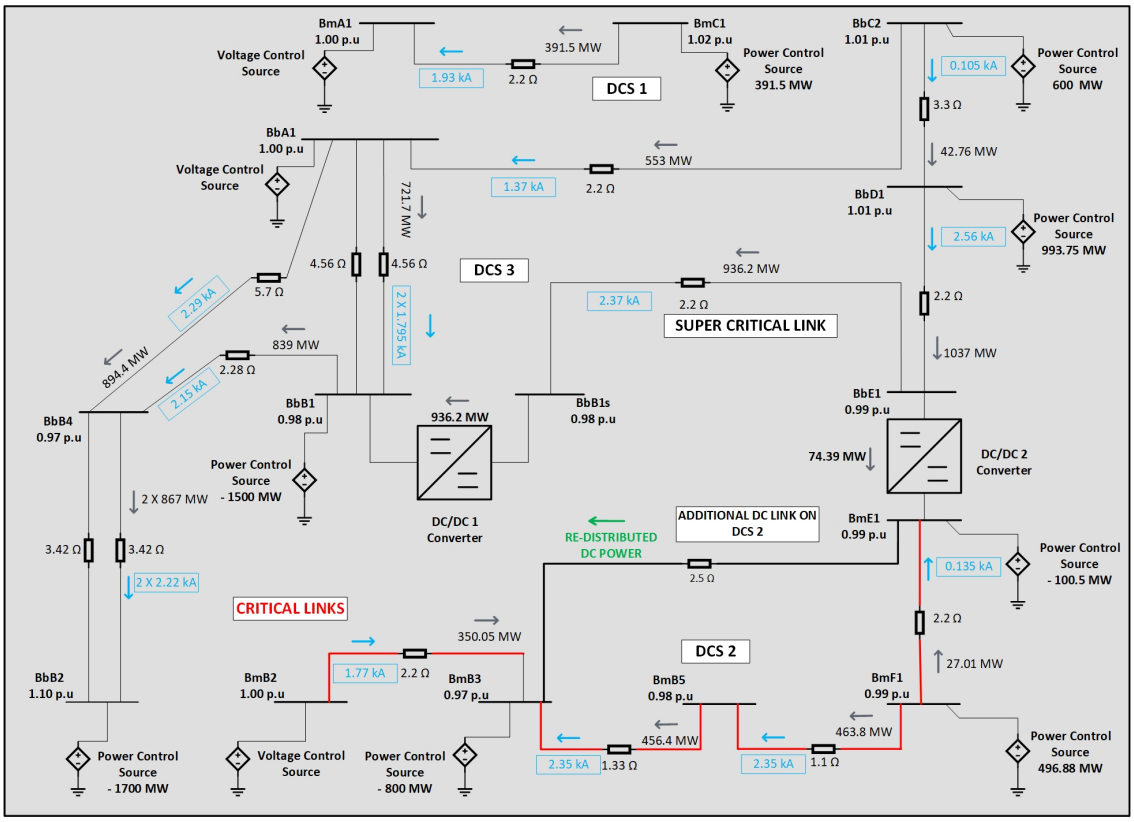

Figure 6.6: DCS 2 Additional DC Link

Initially, a simulation is run with uncontrolled DC/DC converters (modelled as AC transformers with unity turns ratio) instead of the the averaged DC/DC converter model. It was observed that half of the power was re-routed into the additional DC link as per Kirchoff's Current Law (KCL), as would be typically observed in a meshed DC grid.

Correspondingly with inner loop for current control applied on the DC/DC converter, any disconnection of the cascaded DC Links from DC bus BmE1 to BmB3 no longer made the DC grid unstable, as there always was a converter at BmB2 in voltage controlled mode. The power was being redistributed through the additional DC link to the load at bus BmB3. Further, the disconnection of the DC link from BmB3 to BmB2 caused the grid to become unstable due to loss of volage control.

Conclusively, adding a DC link, as shown in Fig. 6.6 from BmE1 to BmB3 provides a bypass DC Link which can promote cascaded *Critical* DC links to being *Non Critical*, and further make the DC grid robust.

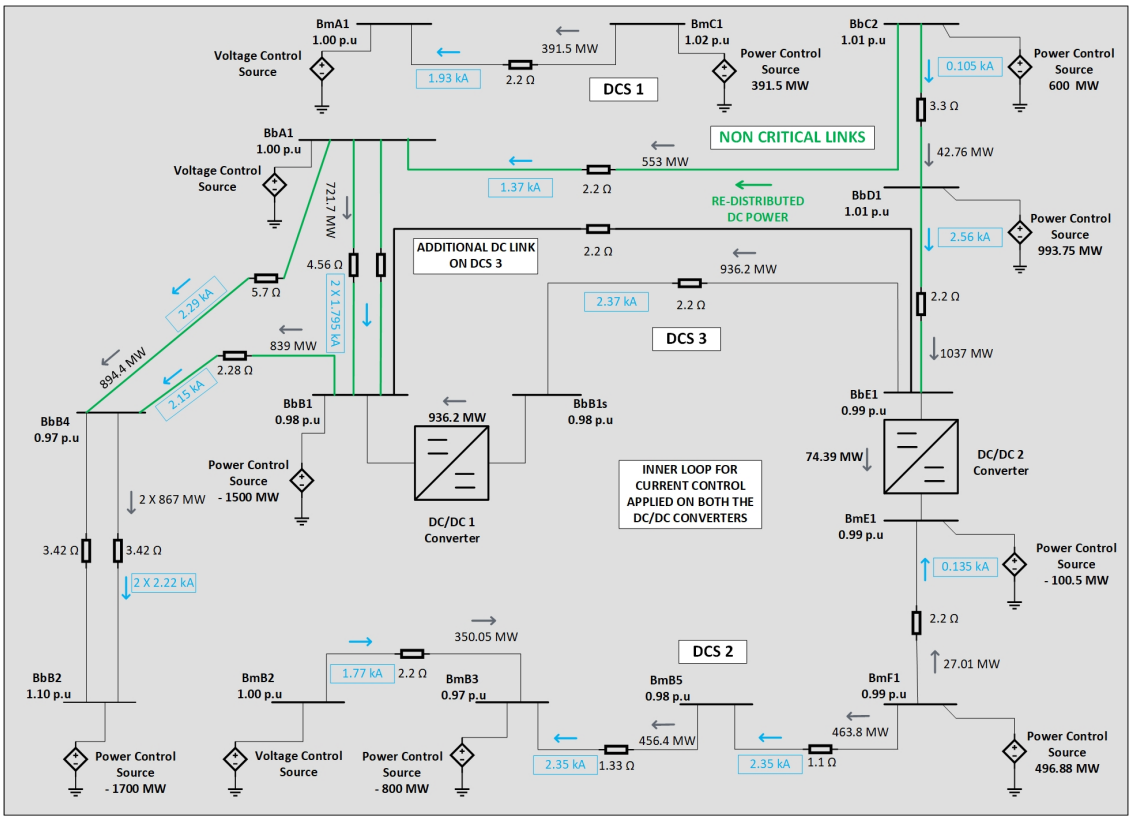

Figure 6.7: DCS 3 Additional DC Link

6.7.2 Additional DC Links in DCS 3 Subsystem

From the steady state contingency analysis conducted in Chapter 5, it was found that all the DC links that were directly connected to a converter at DC bus in voltage control mode were *Non Critical*, while the DC links that were connected to converters at DC buses in power control mode were *Critical*. The disconnection of any of them led to a loss of voltage control which made the DC grid unstable. To further test the system stability with only current control loops, an additional DC Link between the DC/DC converters is implemented. The cable used is a DC symmetrical overhead monopole line. As shown in Figure 6.7, adding a DC link from BbB1 to BbE1 provides a backup DC link for redistributing power between the DC/DC converters.

Similarly, a simulation is run with uncontrolled DC/DC converters. It was observed that power was re-routed into the additional DC link as per KCL, as would be typically observed in a meshed DC grid.

Correspondingly with inner loop for current control applied, any disconnection of the *Critical* DC links no longer caused the grid to become unstable, as the power was being redistributed through the additional DC link from one DC/DC converter to the other.

Conclusively, adding a DC link, as shown in Fig. 6.7 from BbB1 to BbE1 pro-

vides a bypass DC Link which can promote *Critical* DC links to being *Non Critical*, and further make the DC grid robust.

7

Conclusions and Future Work

This chapter summarises conclusions obtained from the thesis work. Further, some suggestions for future research in this topic are introduced.

7.1 Conclusions

In this thesis, DC power flow analysis over the developed model for DC side from CIGRE DC Grid Test System with series embedded DC/DC converters is investigated. Simulations are performed with the objective of developing control strategies for the series embedded DC/DC converters which have been tested and verified for the (n-1) contingency criterion. When compared to an AC system, these control strategies developed for the MTDC grid are analogous to a primary frequency response system. The understandings developed from this thesis are listed below.

- The control strategies designed are reusable in other systems. In the thesis, voltage/current at one end is considered as reference to control the voltage/current over the other end of the DC/DC converter. Since the converters are bi-directional, the control reference can be interchanged.

- The presence of a VSC that is in voltage control mode is essential to maintain DC grid stability and regulate the DC power flow in cases of (n-1) contingencies. If there is no VSC on voltage control mode, the DC/DC converter must be applied with outer loop for voltage control to maintain DC grid stability. Applying only inner loop for current control will lead to DC grid instability, as there is no voltage control to regulate the DC power flow anymore.

- Further, following a *Critical* DC link disconnection in one subsystem, the outer loop for voltage control could be selectively applied only on the DC/DC converter in that subsystem, while inner loop for current control on the DC/DC converter in other subsystems could be sufficient in maintaining DC grid stability. This selective control strategy however is subjective to DC grid topology and the placement of the DC/DC converter in the network.

  In cases where the VSC in voltage control mode is unable to maintain stiff

DC voltage output, modified step control can be implemented wherein a selective loop technique can switch the outer loops between voltage step ratio to voltage control. However, it should be noted that the dynamics of the DC link capacitors can slow down the instability deployment. Therefore, giving time to switch into a suitable control mode can help mitigate the same.

- Once the DC grid has reached steady state following a *Critical* DC link disconnection, a possible solution towards mitigating overloading of the DC links is by varying the power inputs along with step responses from the DC/DC converters.

- Additional DC links can decrease the risk of instability. However, from an economical point of view, manufacturing and maintaining an additional DC Link as compared to a DC/DC converter might not be an intelligible option. Moreover, the integration of additional DC Links to expand the MTDC grid could be done using a DC/DC converter that can provide for a stiff DC voltage at one end.

- In this thesis, contingencies created on the DC Links are only studied through steady state DC power flow analysis. However, the DC protection system must be designed faster than AC protection system to disconnect overloaded DC Links.

7.2 Future Work

Power flow analysis for both DC & AC grids following contingencies when two HVDC systems connected intermediately via an AC link needs to be studied. Further, since the topologies for MTDC grids are theoretical, much research needs to be done regarding DC power flow with different combinations of MTDC grid topologies and control strategies over the DC/DC converters for the stability need to be developed as well.

For AC grids, secondary and tertiary responses have been developed. The same could be needed for the same. It should be noted that the secondary and tertiary response of the MTDC might need to be co-ordinated with the underlying AC system.

Finally, the existing topologies for DC/DC converter take into account the functionality of the converters, while no topology takes into account the adaptability of the control strategy that needs to be applied. Since the DC/DC converters are intended to have fixed topologies, creating mechanical changes to suit control adaptability and economical suitability of doing so needs to be investigated.

Bibliography

[1] S. Chatzivasileiadis, D. Ernst and G. Andersson, "The Global Grid", Arxiv.org, 2018. [Online]. Available: https://arxiv.org/abs/1207.4096.

[2] "Renewables 2017 : Key Findings", Iea.org, 2018. [Online]. Available: https://www.iea.org/publications/renewables2017/.

[3] "More renewables mean less stable grids, researchers find", Powerengineeringint.com, 2018. [Online]. Available: https://www.powerengineeringint.com/articles/2018/01/more-renewables-mean-less-stable-grids-researchers-find.html.

[4] Temesgen M. Haileselassie, Marta Molinas, Tore Undeland, "Multi-Terminal VSC-HVDC System for Integration of Offshore Wind Farms and Green Electrification of Platforms in the North Sea" 2008, Nordic Workshop on Power and Industrial Electronics, June 9-11, 2008.

[5] X. Cheng, M. Korpas, and H. Farahmand, "The impact of electrification on power system in Northern Europe," 2017 14th International Conference on the European Energy Market (EEM), 2017.

[6] J. Robinson, D. Jovcic, and G. Joos, "Analysis and Design of an Offshore Wind Farm Using a MV DC Grid," IEEE Transactions on Power Delivery, vol. 25, no. 4, pp. 2164–2173, 2010.

[7] N. G. Hingorani and L. Gyugyi, Understanding FACTS: concepts and technology of flexible AC transmission systems. Delhi: IEEE Press, 2001.

[8] D. V. Hertem, O. Gomis-Bellmunt, and J. Liang, HVDC grids for offshore and supergrid of the future. Chichester, West Sussex: Wiley Blackwell, Pg 25-41, Chapter 2, 2016.

[9] S. K. Kolparambath, J. A. Suul, and E. Tedeschi, "DC/dc converters for interconnecting independent HVDC systems into multiterminal DC grids," 2015 IEEE 13th Brazilian Power Electronics Conference and 1st Southern Power Electronics Conference (COBEP/SPEC), 2015.

[10] C. D. Barker, C. C. Davidson D. R. Trainer and R. S. Whitehouse. *Requirements of DC/DC Converters to Facilitate Large DC Grids* for Alstom Grid UK Ltd in the United Kingdom in CIGRE by Working Group B4-204, 2012.

[11] C. Sheridan, M. Merlin, and T. Green, "Assessment of DC/DC converters for use in DC nodes for offshore grids," 10th IET International Conference on AC and DC Power Transmission (ACDC 2012), 2012.

[12] D. Jovcic, D. V. Hertem, K. Linden, J.-P. Taisne, and W. Grieshaber, "Feasibility of DC transmission networks," 2011 2nd IEEE PES International Conference and Exhibition on Innovative Smart Grid Technologies, 2011.

[13] G. Stamatiou and M. Bongiorno, "A novel decentralized control strategy for MultiTerminal HVDC transmission grids," 2015 IEEE Energy Conversion Congress and Exposition (ECCE), 2015.

[14] F. Thams, J. A. Suul, S. Darco, M. Molinas, and F. W. Fuchs, "Stability of DC voltage droop controllers in VSC HVDC systems," 2015 IEEE Eindhoven PowerTech, 2015.

[15] G. Stamatiou and M. Bongiorno, "Power-dependent droop-based control strategy for multi-terminal HVDC transmission grids," IET Generation, Transmission & Distribution, Nov. 2016.

[16] T. M. Haileselassie and K. Uhlen, "Precise control of power flow in multiterminal VSC-HVDCs using DC voltage droop control," 2012 IEEE Power and Energy Society General Meeting, 2012.

[17] T. M. Haileselassie and K. Uhlen, "Primary frequency control of remote grids connected by multi-terminal HVDC," IEEE PES General Meeting, 2010.

[18] L. Xu, L. Yao, and M. Bazargan, “DC grid management of a multi-terminal HVDC transmission system for large offshore wind farms,” 2009 International Conference on Sustainable Power Generation and Supply, 2009.

[19] G. P. Adam, S. J. Finney, B. W. Williams, D. Holliday, and I. A. Gowaid, “Review of dc–dc converters for multi-terminal HVDC transmission networks,” IET Power Electronics, vol. 9, no. 2, pp. 281–296, Oct. 2016.

[20] Piwko, R., Miller, N., Sanchez-Gasca, J., Yuan, X., Dai, R. and Lyons, J. (2009). Integrating Large Wind Farms into Weak Power Grids with Long Transmission Lines - IEEE Conference Publication. [online] Ieeexplore.ieee.org. Available at: https://ieeexplore.ieee.org/stamp/stamp.jsp?tp=&arnumber=4778165 [Accessed 11 Sep. 2018].

[21] D. V. Hertem, O. Gomis-Bellmunt, and J. Liang, HVDC grids for offshore and supergrid of the future. Chichester, West Sussex: Wiley Blackwell, Pg 143-170 , Chapter 7, 2016.

[22] D. V. Hertem, O. Gomis-Bellmunt, and J. Liang, HVDC grids for offshore and supergrid of the future. Chichester, West Sussex: Wiley Blackwell, Pg 171-191 , Chapter 8, 2016.

[23] G. Pinares, “Analysis of the DC dynamics of VSC-HVDC systems connected to weak AC grids using a frequency domain approach,” 2014 Power Systems Computation Conference, 2014.

[24] N.Macleod, J.Liang, "Designing HVDC grids for optimal reliability and availability performance", e-cigré, 2018. [Online]. Available: https://e-cigre.org/publication/713-designing-hvdc-grids-for-optimal-reliability-and-availability-performance.

[25] K. Linden and J. Beerten, "Control methodologies for direct voltage and power flow in a meshed HVDC grid", e-cigré, 2018. [Online]. Available: https://e-cigre.org/publication/699-control-methodologies-for-direct-voltage-and-power-flow-in-a-meshed-hvdc-grid.

[26] X. Li, Z. Yuan, J. Fu, Y. Wang, T. Liu, and Z. Zhu, "Nanao multi-terminal VSC-HVDC project for integrating large-scale wind generation," 2014 IEEE PES General Meeting | Conference & Exposition, 2014.

[27] T. K. Vrana, Y. Yang, D. Jovcic, S. Denneti'ere, J. Jardini and H. Saad, "The CIGRE B4 DC grid test system," Electra, vol. 270, pp. 10–19, 2013.

[28] D. V. Hertem, O. Gomis-Bellmunt, and J. Liang, HVDC grids for offshore and supergrid of the future. Chichester, West Sussex: Wiley Blackwell, Pg 315-331 , Chapter 15, 2016.

[29] Kundur, P., Balu, N. and Lauby, M. (2009). Power system stability and control. New York: McGraw-Hill.

[30] ENTSOE Borchure, Svenska Kraftnet, Nordic Balancing Philosophy, Pg 3-4, 2016.

[31] B. C. Kuo, Automatic control system. New Delhi, India: Prentice Hall, Pg 443-577, Chapter 10, 1970.

[32] Chapman, S. (2012). Electric machinery fundamentals. New York, N.Y.: McGraw-Hill.

A

Appendix A

A.1 DC Control Bus implemented in PSCAD

In PSCAD simulations, to create a power controlled DC bus that would be equivalent to a VSC, a PI controller was used, as shown in Figure A.1. The power input from the DC bus (as a product of voltage and current) is provided as an input signal. This signal is compared with the reference signal given through a signal comparative as pre-decided power set-point. The corrected output is given a voltage summation and is further given to the voltage controlled DC bus in the grid as a control signal.

The power set-point provided is either positive or negative, depending if the VSC is injecting or drawing power.

A.2 DC/DC converter Averaged Model implemented in PSCAD

In PSCAD simulations, the averaged model for the DC/DC converter is implemented as shwon in Figure A.2 and Figure A.3.

A.3 DC Grid Model implemented in PSCAD

Figure A.4 shows the DC grid model implemented in PSCAD.

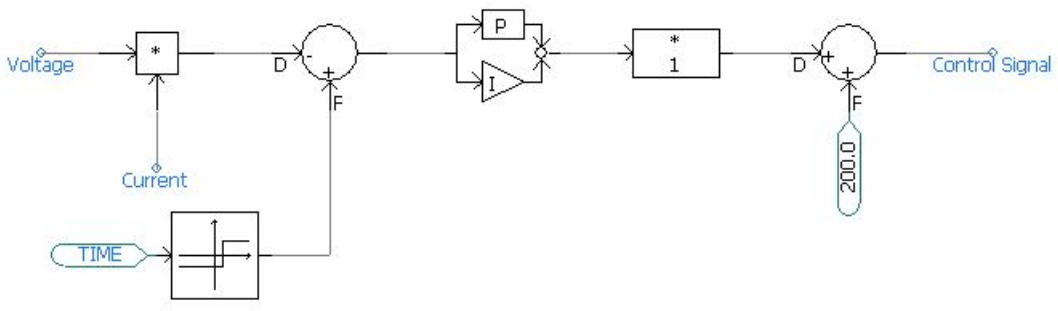

Figure A.1: DC Control Bus in PSCAD

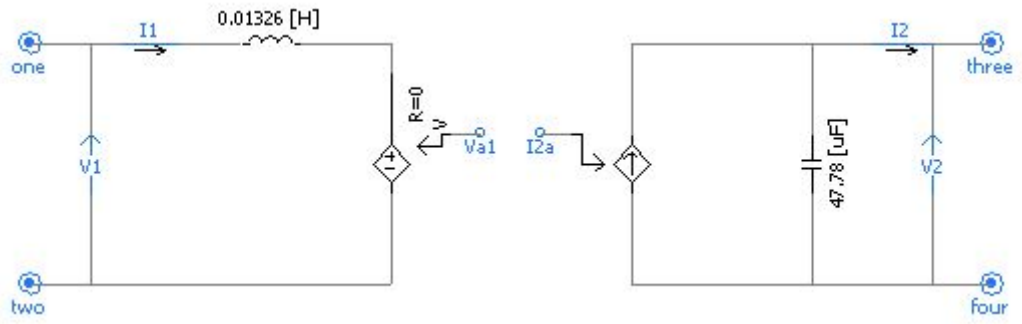

Figure A.2: DC/DC 1 Averaged Model

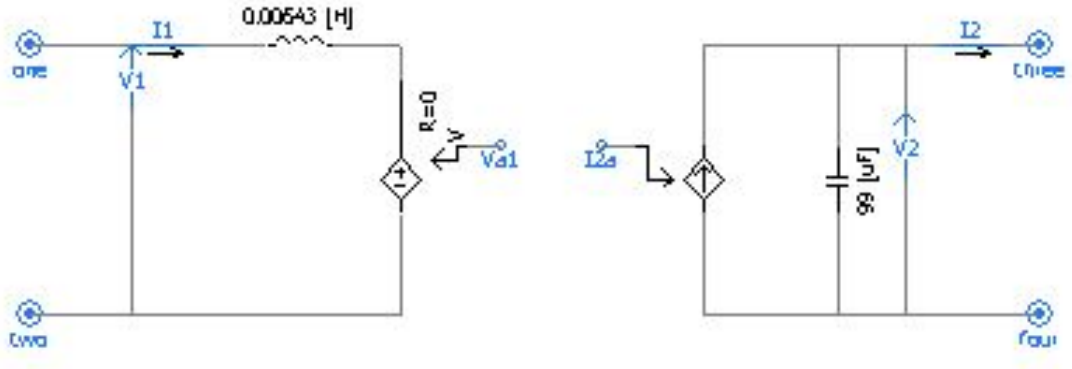

Figure A.3: DC/DC 2 Averaged Model

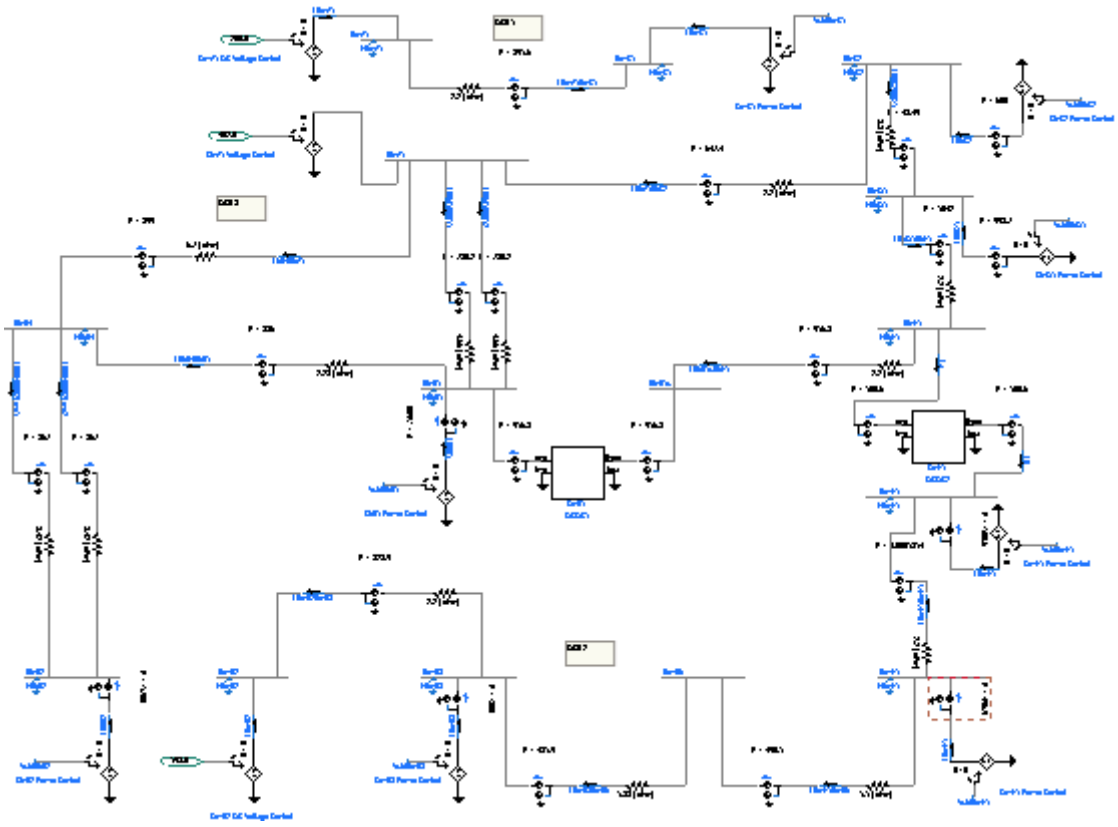

Figure A.4: DC Grid Model in PSCAD

A.4 Inner Loop in PSCAD

In PSCAD simulations, the inner loop for current control uses a PI controller that corrects the error signal derived from the reference and the actual input. The reference input is a set-point current given through a signal comparator and the actual input is a current signal from the grid. Further, the corrected signal is multiplied by a voltage so that it can be fed at the V_a1_1 terminal of the averaged model. In case of DC/DC 2 converter, the corrected signal is multiplied by 2, since its a step-down converter.

A.5 Outer Loop in PSCAD

A.5.0.1 Voltage Control

In PSCAD simulations, the outer loop for voltage control uses cascaded PI controllers that corrects the error signal derived from the reference and the actual input. The reference input is a set-point voltage given through a signal comparator and the actual input is a voltage signal from the grid. Further, the corrected signal is multiplied by a voltage so that it can be fed at the V_a1_1 terminal of the averaged model. In case of DC/DC 2 converter, the corrected signal is multiplied by 2, since its a step-down converter.

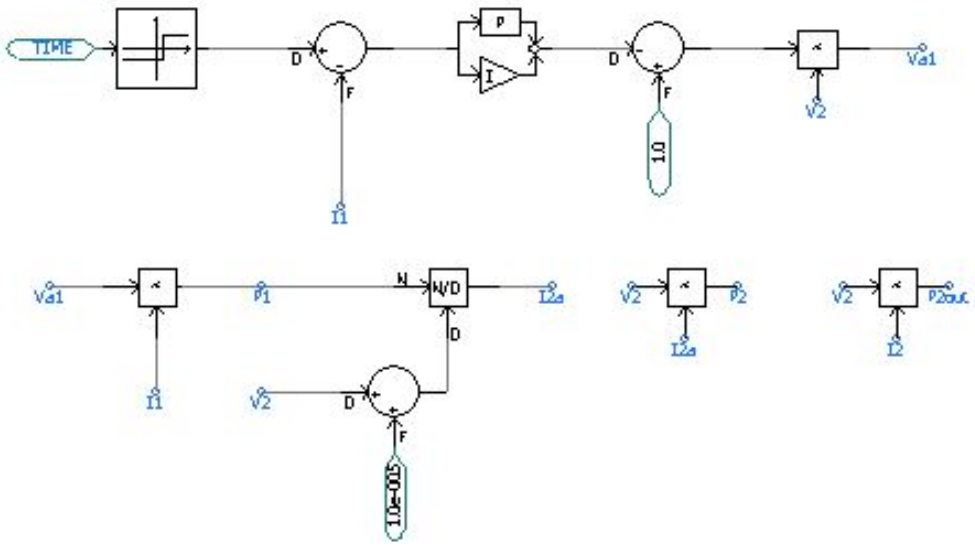

Figure A.5: Inner Loop for DC/DC1

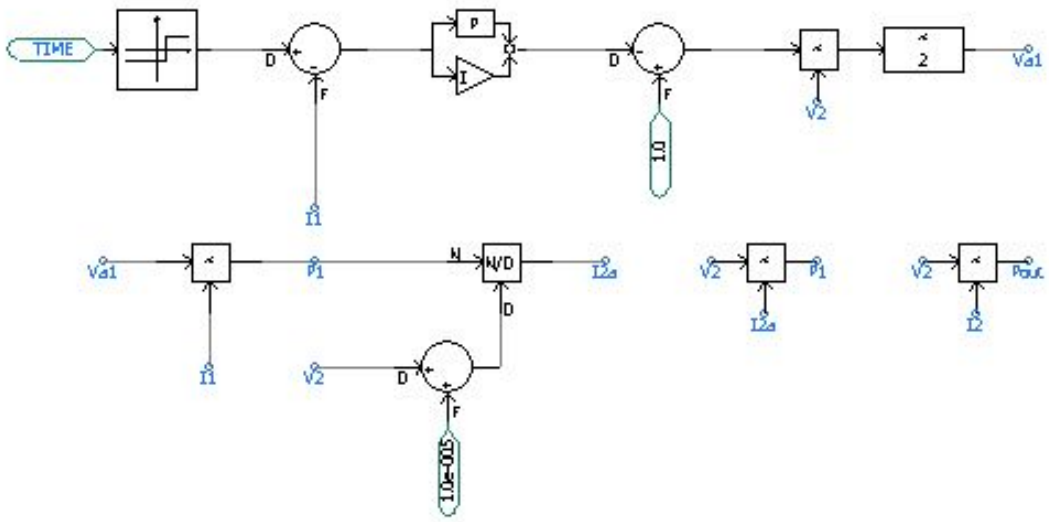

Figure A.6: Inner Loop for DC/DC 2

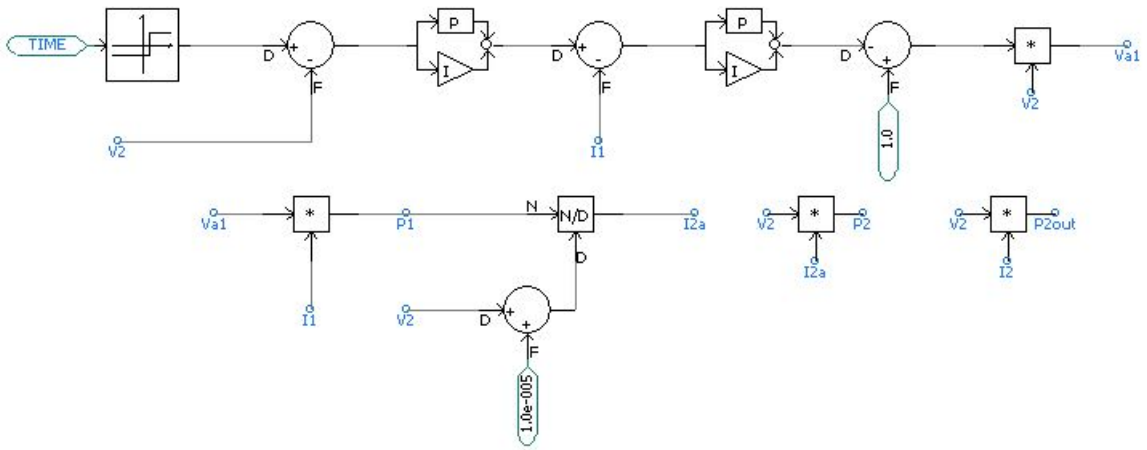

Figure A.7: Outer Loop for DC/DC 1 with Voltage Control

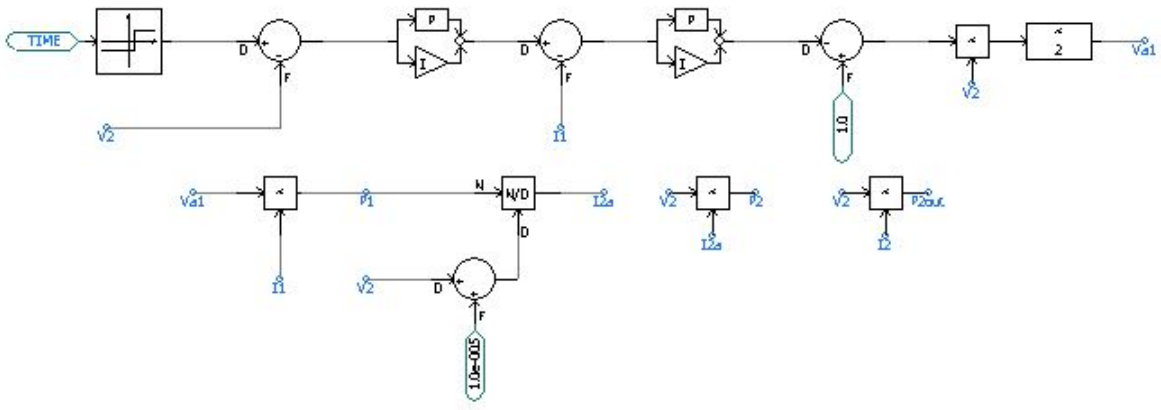

Figure A.8: Outer Loop for DC/DC 2 with Voltage Control

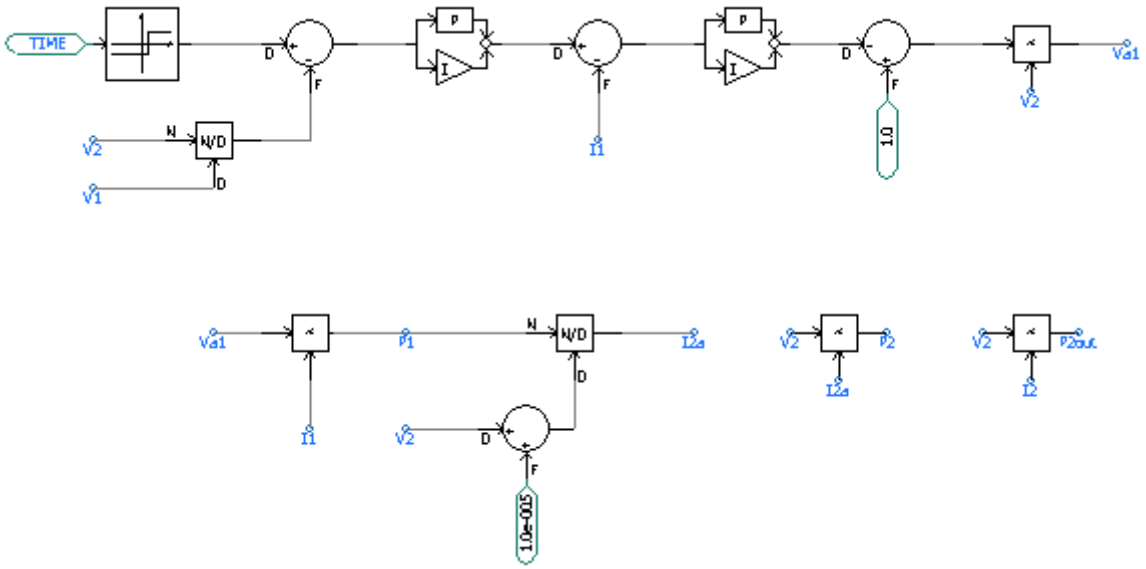

Figure A.9: Outer Loop for DC/DC 1 with Voltage Step Control

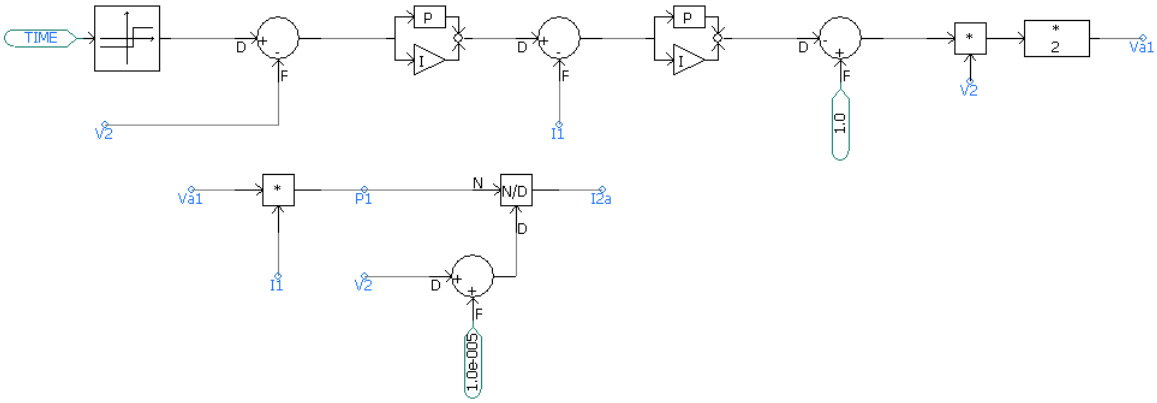

Figure A.10: Outer Loop for DC/DC 2 with Voltage Step Control

A.5.0.2 Voltage Step Ratio Control

In PSCAD simulations, the outer loop for voltage step ratio control uses cascaded PI controllers that corrects the error signal derived from the reference and the actual input. The reference input is a set-point voltage given through a signal comparator and the actual input is the ratio of both the voltage signals from the grid. Further, the corrected signal is multiplied by a voltage so that it can be fed at the V_a1_1 terminal of the averaged model. In case of DC/DC 2 converter, the corrected signal is multiplied by 2, since its a step-down converter and the voltage ratio is maintained to 0.5 as well.

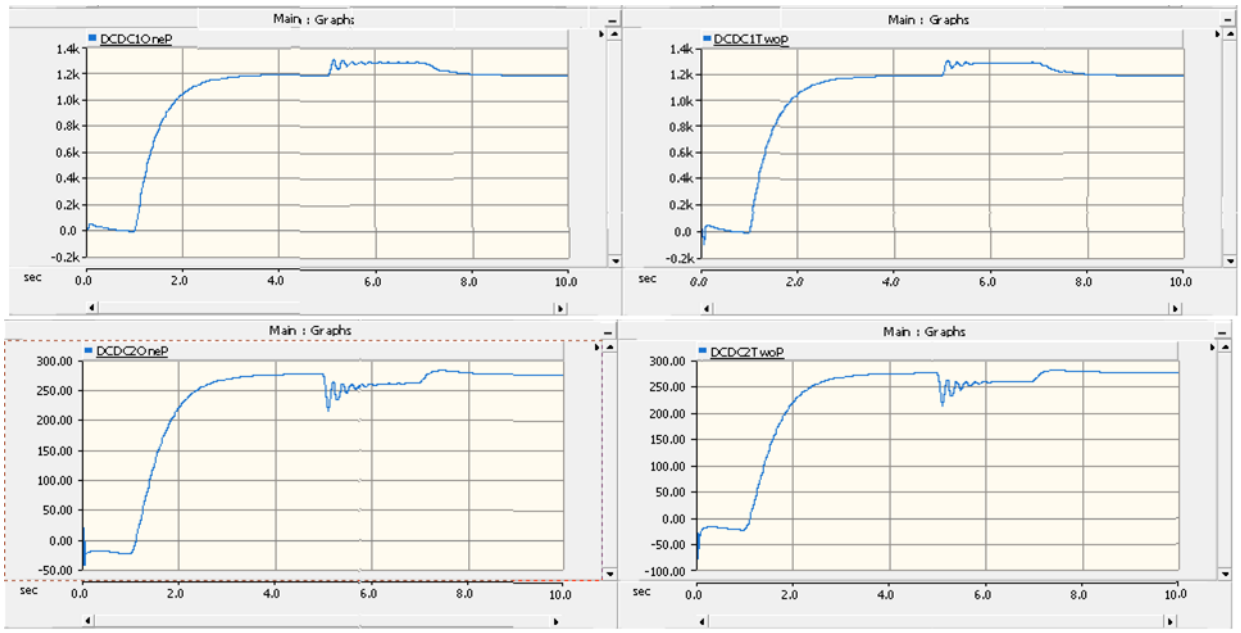

Figure A.11: Typical Output Graphs for VSR Control

A.6 Output Graphs for Voltage Step Ratio Control

Figure A.11 shows a typical DC/DC converter output with voltage step ratio control applied. Oscillations before the steady state can be observed.